



# Latest Results on Reactor Antineutrino Disappearance at Daya Bay

Karsten M. Heeger  
Yale University

*On behalf of the Daya Bay Collaboration*

Yale, September 30, 2013

# Reactor Neutrinos

2012 - Measurement of  $\theta_{13}$   
with Reactor Neutrinos

2008 - Precision measurement of  $\Delta m_{12}^2$ . Evidence for oscillation

2003 - First observation of reactor antineutrino disappearance



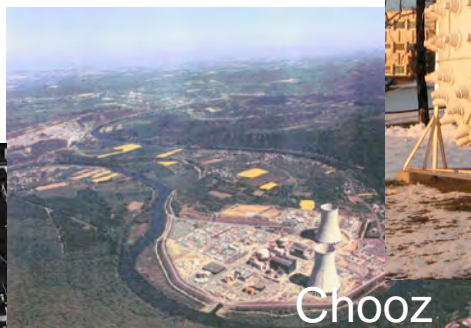
1995 - Nobel Prize to Fred Reines at UC Irvine

1980s & 1990s - Reactor neutrino flux measurements in U.S. and Europe

1956 - First observation of (anti)neutrinos



Savannah River



Chooz



Chooz



KamLAND



## Past Reactor Experiments

- Hanford
- Savannah River
- ILL, France
- Bugey, France
- Rovno, Russia
- Goesgen, Switzerland
- Krasnoyarsk, Russia
- Palo Verde
- Chooz, France

55 years of liquid scintillator detectors  
a story of varying baselines...

# Reactor Antineutrinos

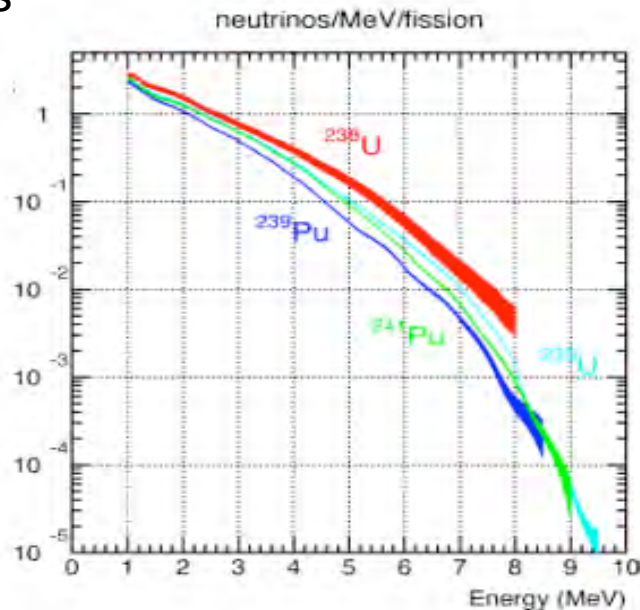
## Source

$\bar{\nu}_e$  from  $\beta$ -decays  
of n-rich fission products



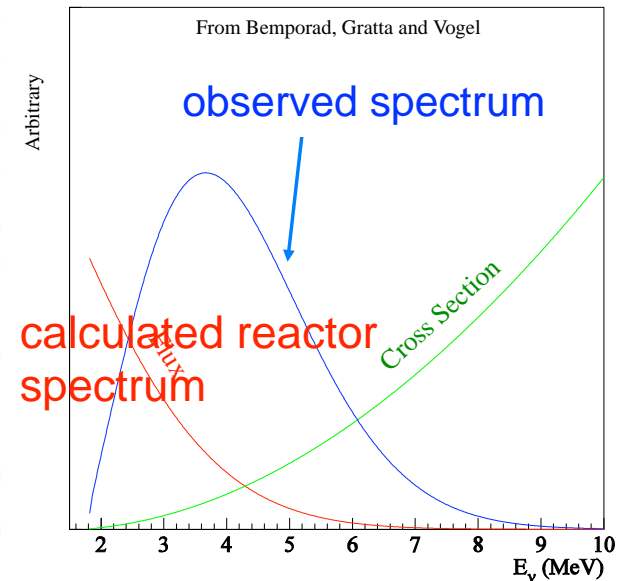
pure  $\bar{\nu}_e$  source

> 99.9% of  $\bar{\nu}_e$  are produced by fissions in  $^{235}\text{U}$ ,  
 $^{238}\text{U}$ ,  $^{239}\text{Pu}$ ,  $^{241}\text{Pu}$



## Detection

inverse beta decay  
 $\bar{\nu}_e + p \rightarrow e^+ + n$



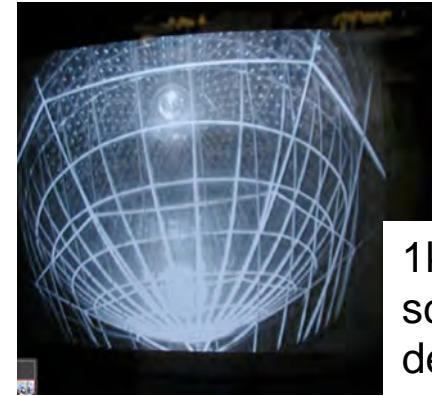
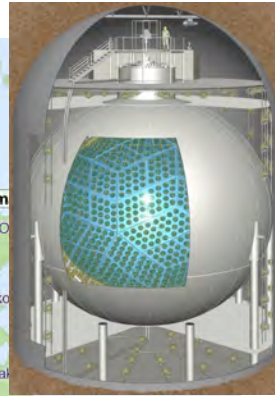
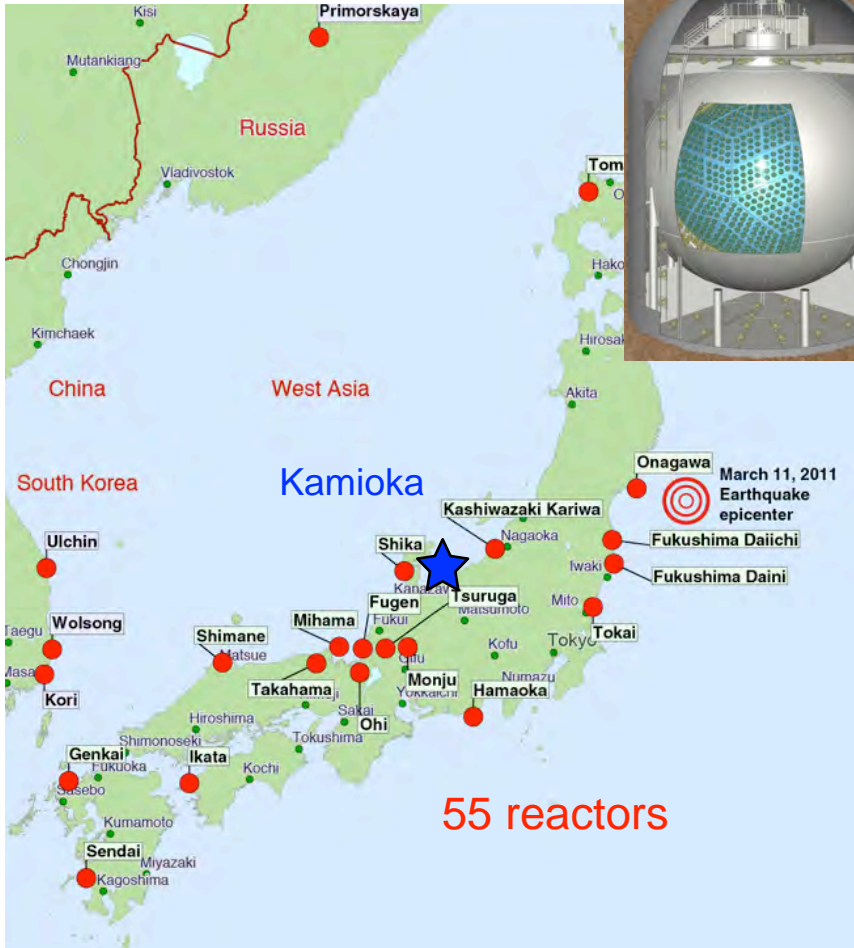
mean energy of  $\bar{\nu}_e$ : 3.6 MeV

only disappearance  
experiments possible

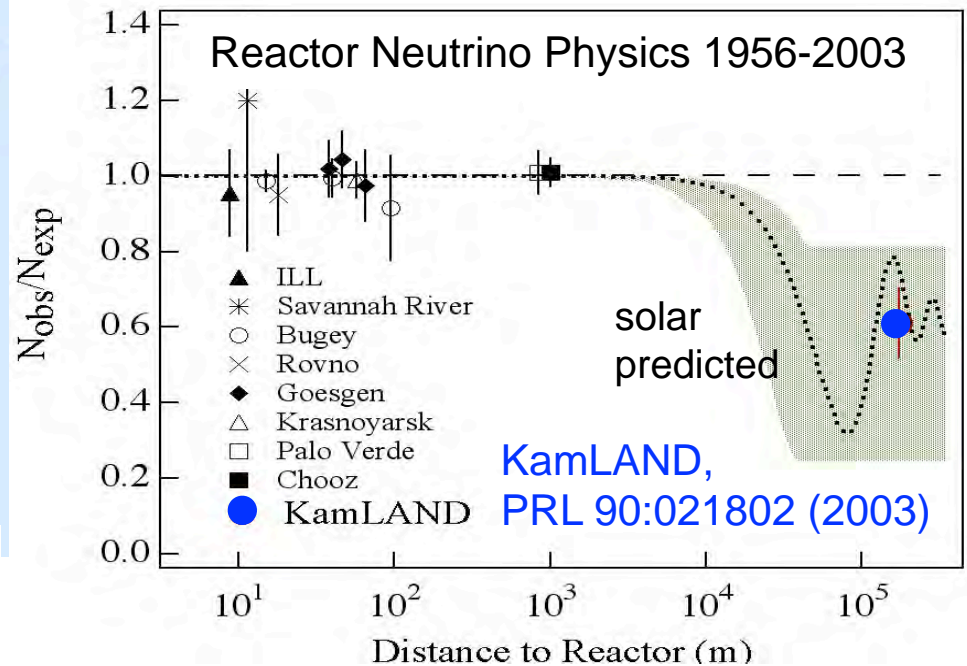
# Observation of Reactor $\bar{\nu}_e$ Disappearance



## KamLAND 2003



1kt liquid scintillator detector

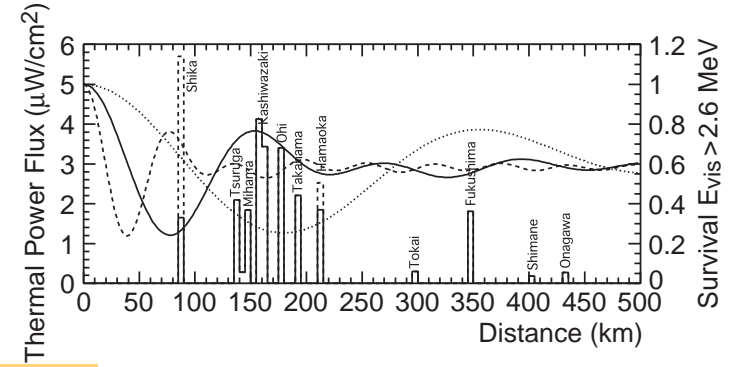
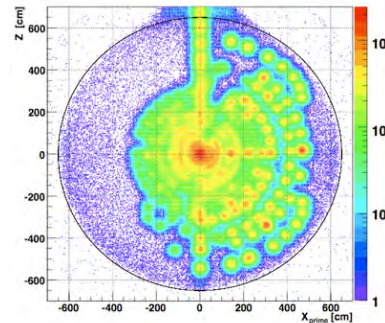
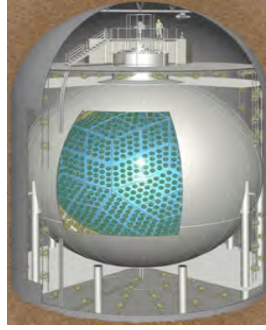


mean, flux-weighted reactor distance  
~ 180km

# Reactor Antineutrinos at KamLAND

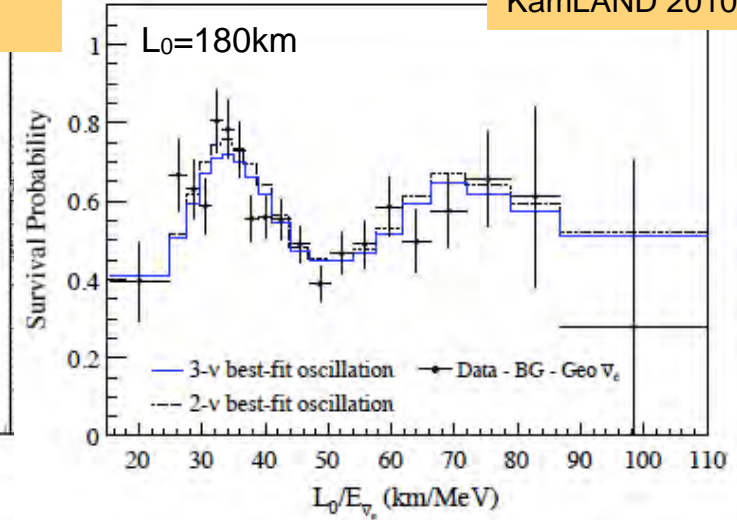
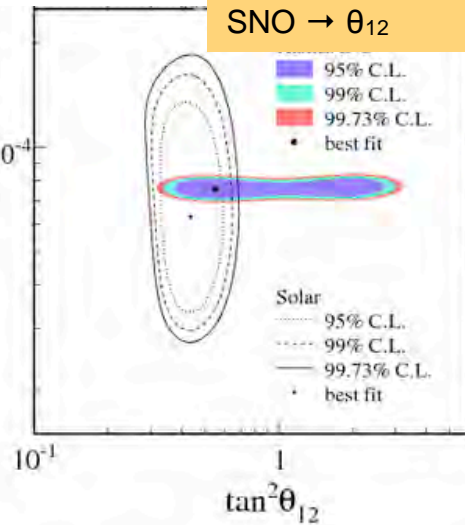
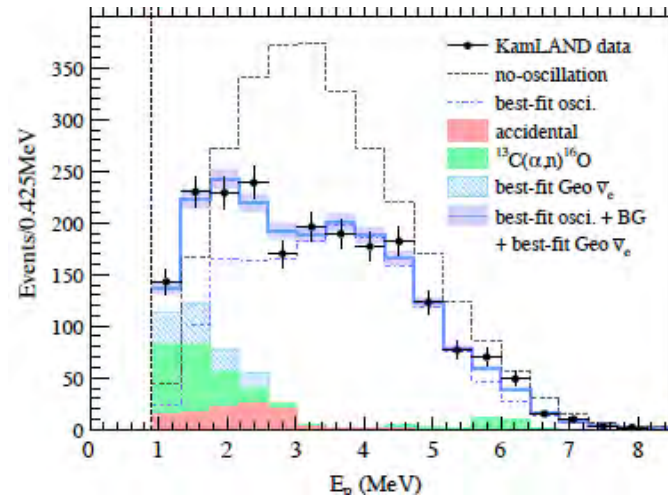


## KamLAND 2007-2010



KamLAND →  $\Delta m_{12}^2$   
SNO →  $\theta_{12}$

KamLAND 2010



Evidence for spectral distortion

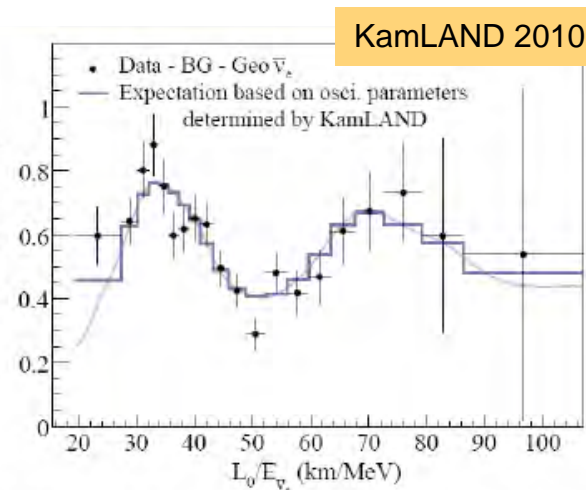
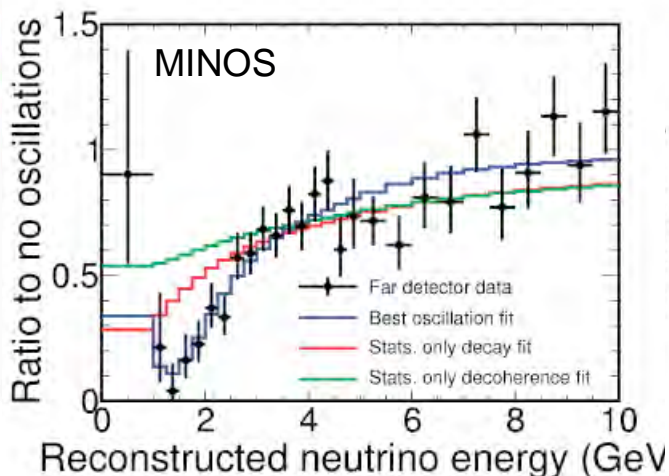
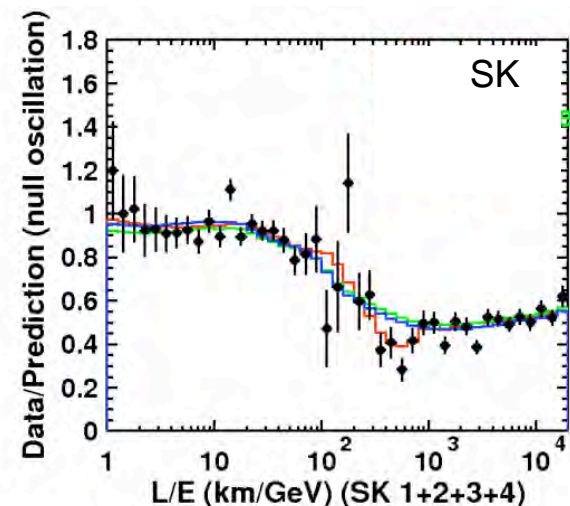
KamLAND has measured  $\Delta m_{12}^2$  to  $\sim 2.8\%$

Direct evidence for oscillation

# Neutrino Oscillation Measurements

## Recent Observations

- atmospheric  $\nu_\mu$  and  $\bar{\nu}_\mu$  disappear most likely to  $\nu_\tau$  (SK, MINOS)
- accelerator  $\nu_\mu$  and  $\bar{\nu}_\mu$  disappear at  $L \sim 250, 700$  km (K2K, T2K, MINOS)
- some accelerator  $\nu_\mu$  appear as  $\nu_\mu$  at  $L \sim 250, 700$  km (T2K, MINOS)
- solar  $\nu_e$  convert to  $\nu_\mu/\nu_\tau$  (Cl, Ga, SK, SNO, Borexino)
- reactor  $\bar{\nu}_e$  disappear at  $L \sim 200$  km (KamLAND)
- reactor  $\bar{\nu}_e$  disappear at  $L \sim 1$  km (DC, Daya Bay, RENO)



Experiments have demonstrated vacuum oscillation L/E pattern

$$P_{i \rightarrow i} = \sin^2 2\theta \sin^2 \left( 1.27 \Delta m^2 \frac{L}{E} \right)$$

# Neutrino Oscillation

## Neutrino Oscillation Imply Neutrino Mass

mass eigenstates  $\neq$  flavor eigenstates

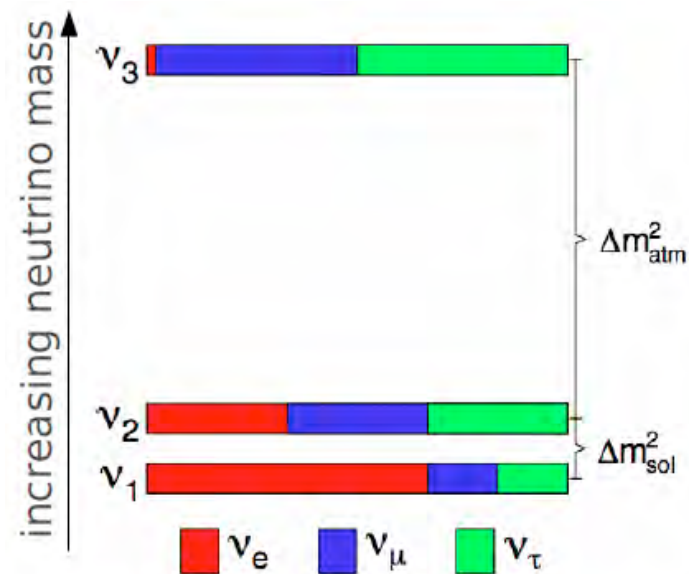
$$|\nu_\alpha\rangle = \sum_i U_{\alpha i}^* |\nu_i\rangle$$

flavor composition of neutrinos changes as they propagate

$$\begin{aligned}
 P(\nu_\alpha \rightarrow \nu_\beta) &= |\langle \nu_\beta | \nu_\alpha(L) \rangle|^2 \\
 &= \delta_{\alpha\beta} - 4 \sum_{i>j} \Re(U_{\alpha i}^* U_{\beta i} U_{\alpha j} U_{\beta j}^*) \sin^2[1.27 \Delta m_{ij}^2 L/E] \\
 &\quad + 2 \sum_{i>j} \Im(U_{\alpha i}^* U_{\beta i} U_{\alpha j} U_{\beta j}^*) \sin^2[2.54 \Delta m_{ij}^2 L/E]
 \end{aligned}$$

2-neutrino case

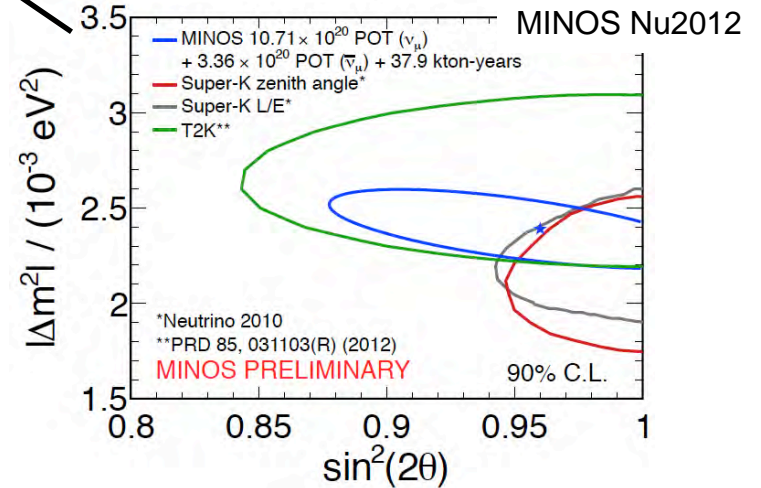
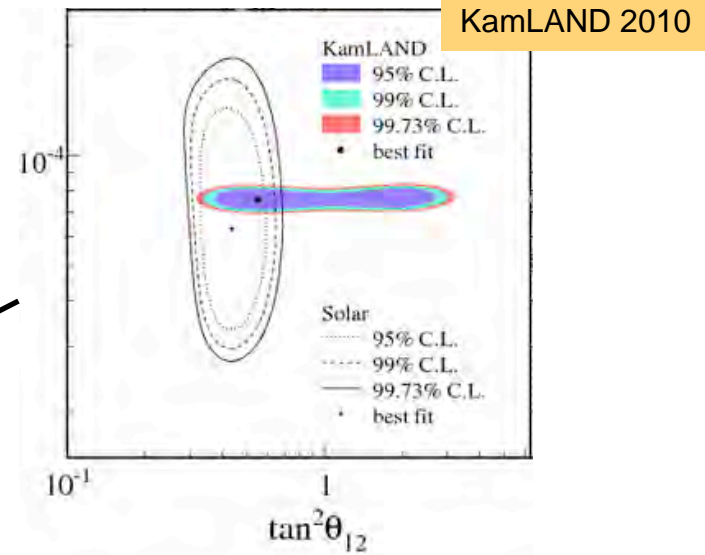
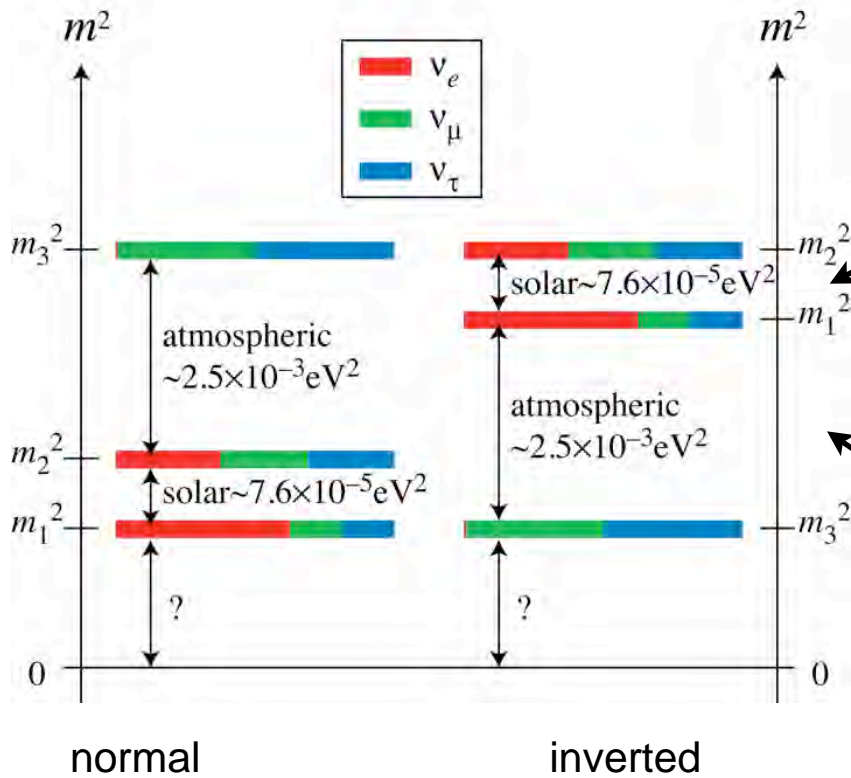
$$P_{i \rightarrow j} = \sin^2 2\theta \sin^2 \left( 1.27 \Delta m^2 \frac{L}{E} \right)$$



energy and baseline dependent  
osc frequency depends on  $\Delta m^2$   
amplitude depends on  $\theta$

# Measurement of Fundamental Parameters

## Mass Splittings



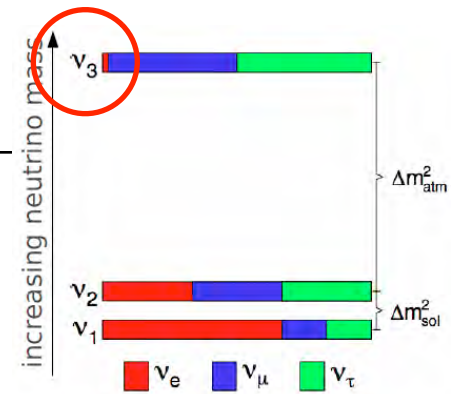


# Neutrino Oscillation - Before 2011

## Mixing Angles

$$U = \begin{pmatrix} U_{e1} & U_{e2} & U_{e3} \\ U_{\mu 1} & U_{\mu 2} & U_{\mu 3} \\ U_{\tau 1} & U_{\tau 2} & U_{\tau 3} \end{pmatrix} = \begin{pmatrix} 0.8 & 0.5 & U_{e3} \\ 0.4 & 0.6 & 0.7 \\ 0.4 & 0.6 & 0.7 \end{pmatrix} \quad U_{\text{MNSP}} \text{ Matrix}$$

Maki, Nakagawa, Sakata, Pontecorvo



$$= \underbrace{\begin{pmatrix} 1 & 0 & 0 \\ 0 & \cos\theta_{23} & \sin\theta_{23} \\ 0 & -\sin\theta_{23} & \cos\theta_{23} \end{pmatrix}}_{\text{atmospheric, K2K}} \times \underbrace{\begin{pmatrix} \cos\theta_{13} & 0 & e^{-i\delta_{CP}} \sin\theta_{13} \\ 0 & 1 & 0 \\ -e^{i\delta_{CP}} \sin\theta_{13} & 0 & \cos\theta_{13} \end{pmatrix}}_{\text{reactor and accelerator}} \times \underbrace{\begin{pmatrix} \cos\theta_{12} & \sin\theta_{12} & 0 \\ -\sin\theta_{12} & \cos\theta_{12} & 0 \\ 0 & 0 & 1 \end{pmatrix}}_{\text{SNO, solar SK, KamLAND}} \times \underbrace{\begin{pmatrix} 1 & 0 & 0 \\ 0 & e^{i\alpha/2} & 0 \\ 0 & 0 & e^{i\alpha/2+i\beta} \end{pmatrix}}_{\text{0}\nu\beta\beta}$$

atmospheric, K2K

reactor and accelerator

SNO, solar SK, KamLAND

$0\nu\beta\beta$

$$\sin^2 \theta_{23}$$

$$\sin^2 \theta_{13}$$

$$\sin^2 \theta_{12}$$

$$0.50^{+0.07}_{-0.06}$$

small? zero?

$$0.318^{+0.019}_{-0.016}$$

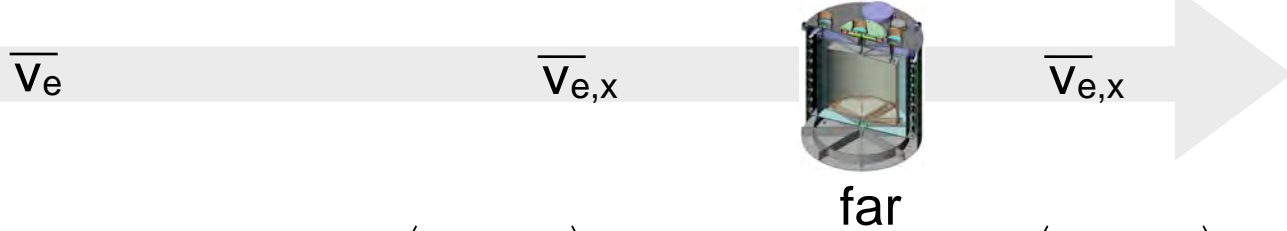
maximal?

large, but not maximal!

# Reactor Neutrino Oscillation Experiments



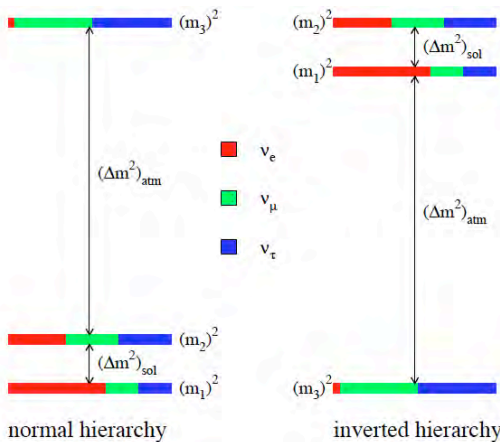
Measure (non)- $1/r^2$  behavior of  $\bar{\nu}_e$  interaction rate



$$P_{ee} \approx 1 - \sin^2 2\theta_{13} \sin^2 \left( \frac{\Delta m_{31}^2 L}{4E_\nu} \right) - \cos^4 \theta_{13} \sin^2 2\theta_{12} \sin^2 \left( \frac{\Delta m_{21}^2 L}{4E_\nu} \right)$$

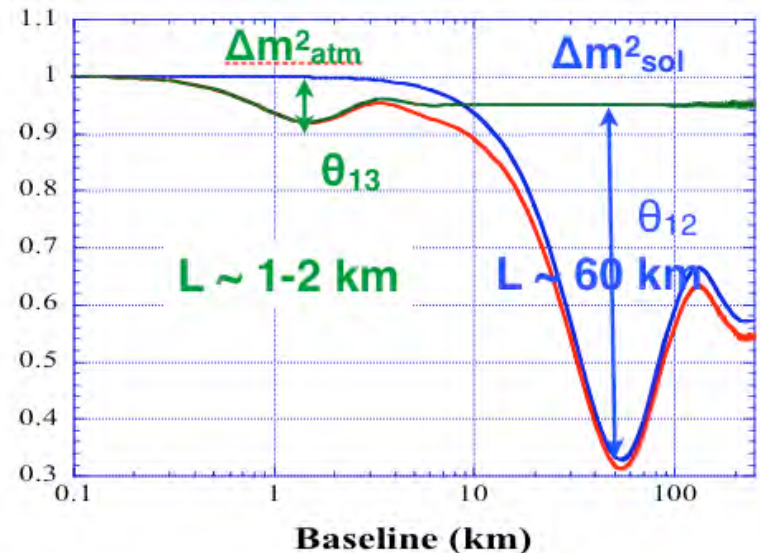
for 3 active  $\nu$ , two different oscillation length scales:  $\Delta m^2_{12}, \Delta m^2_{23}$

$L/E \rightarrow \Delta m^2$  amplitude of oscillation  $\rightarrow \theta$



$$\Delta m^2_{12} \sim 7.6 \times 10^{-5} \text{ eV}^2$$

$$\Delta m^2_{23} \sim 2.4 \times 10^{-3} \text{ eV}^2$$



# Measuring $\theta_{13}$ with Reactor Experiments

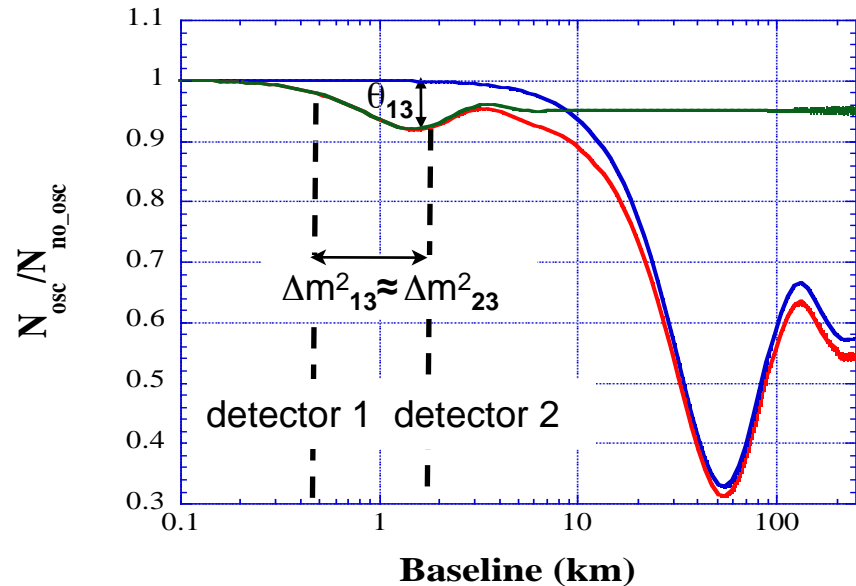
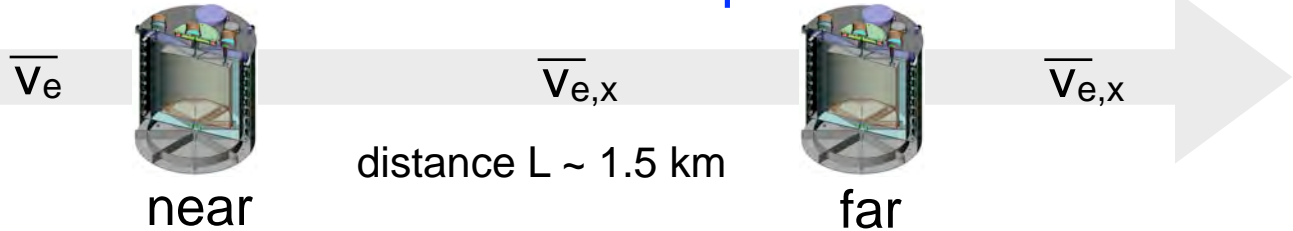


**Absolute Reactor Flux**  
Largest uncertainty in previous measurements

**Relative Measurement**  
Removes absolute uncertainties!

First proposed by L. A. Mikaelyan and V.V. Sinev,  
Phys. Atomic Nucl. 63 1002 (2000)

## Near-Far Concept



$$\frac{N_f}{N_n} = \left( \frac{N_{p,f}}{N_{p,n}} \right) \left( \frac{L_n}{L_f} \right)^2 \left( \frac{\epsilon_f}{\epsilon_n} \right) \left[ \frac{P_{\text{sur}}(E, L_f)}{P_{\text{sur}}(E, L_n)} \right]$$

far/near  $\bar{V}_e$  ratio

target mass

distances

efficiency

oscillation deficit

# Daya Bay Nuclear Power Plant



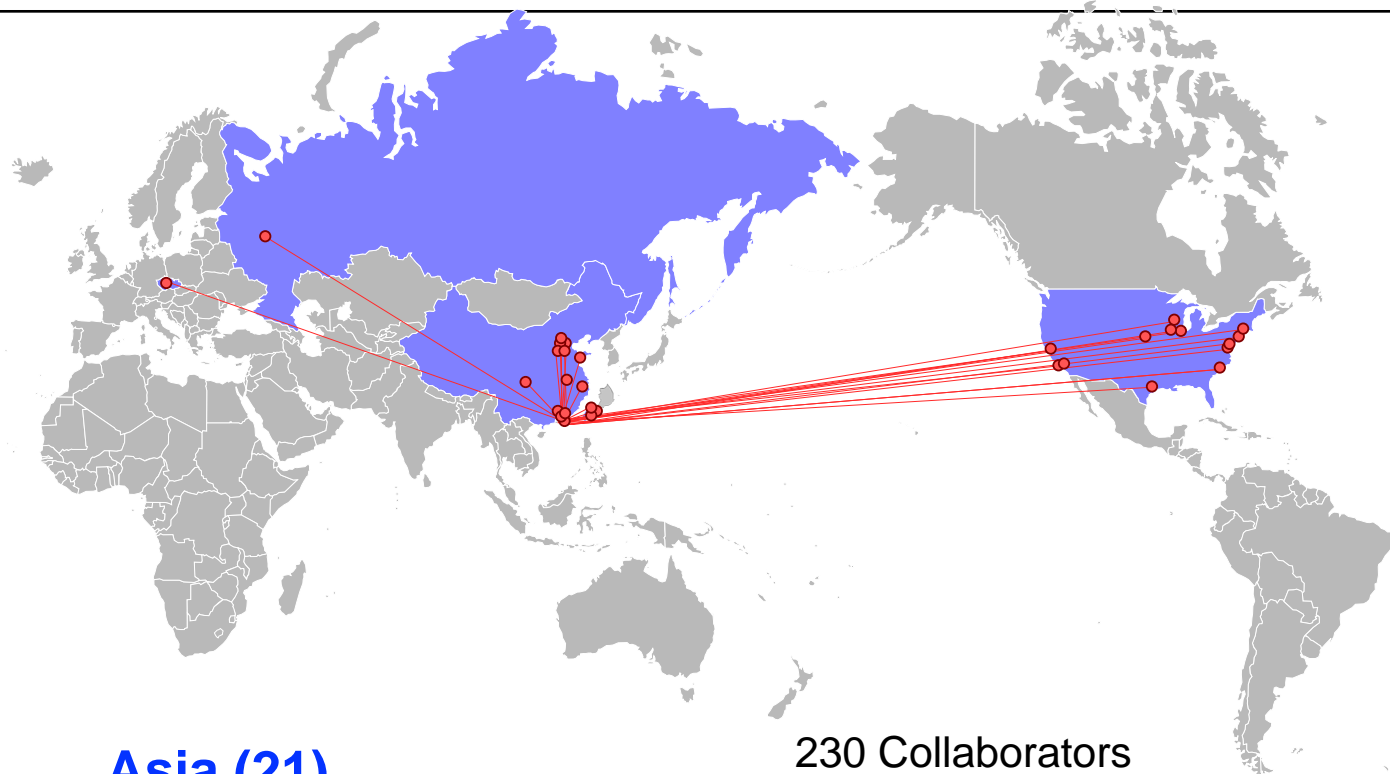
## A Powerful Neutrino Source

- Among the top 5 most powerful reactor complexes in the world, producing  $17.4 \text{ GW}_{\text{th}}$  ( $6 \times 2.95 \text{ GW}_{\text{th}}$ )
- All 6 reactors are in commercial operation
- Adjacent to mountains; convenient to construct tunnels and underground labs with sufficient overburden to suppress cosmic rays



Reactors produce  $\sim 2 \times 10^{20}$  antineutrinos/sec/GW

# An International Effort



## Asia (21)

Beijing Normal Univ., CGNPG, CIAE, Dongguan Polytechnic, ECUST, IHEP, Nanjing Univ., Nankai Univ., NCEPU, Shandong Univ., Shanghai Jiao Tong Univ., Shenzhen Univ., Tsinghua Univ., USTC, Xian Jiaotong Univ., Zhongshan Univ., Chinese Univ. of Hong Kong, Univ. of Hong Kong, National Chiao Tung Univ., National Taiwan Univ., National United Univ.

## Europe (2)

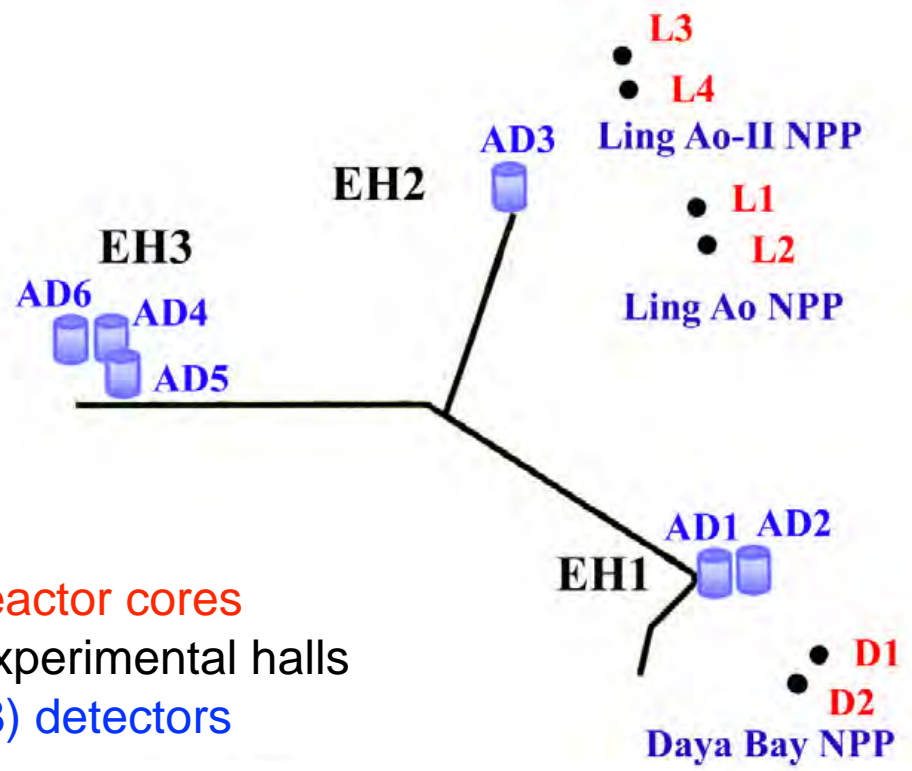
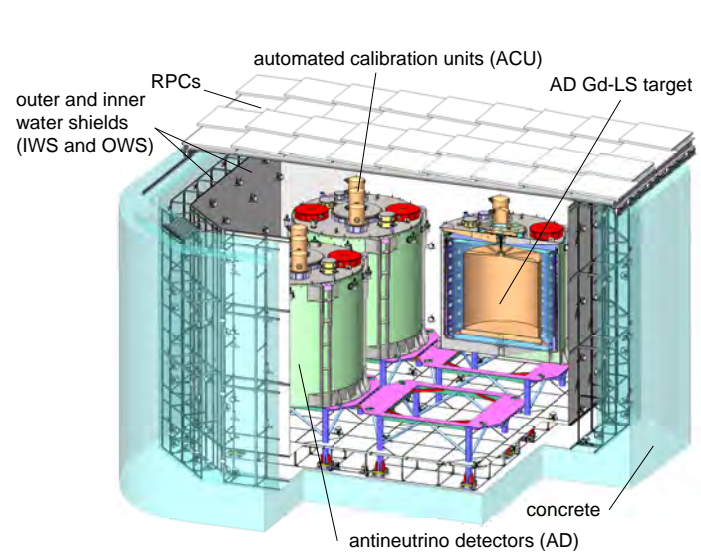
Charles University, JINR Dubna

230 Collaborators  
from 40 Institutions

## North America (17)

Brookhaven Natl Lab, CalTech, Illinois Institute of Technology, Iowa State, Lawrence Berkeley Natl Lab, Princeton, Rensselaer Polytechnic, Siena College, UC Berkeley, UCLA, Univ. of Cincinnati, Univ. of Houston, UIUC, Univ. of Wisconsin, Virginia Tech, William & Mary, Yale

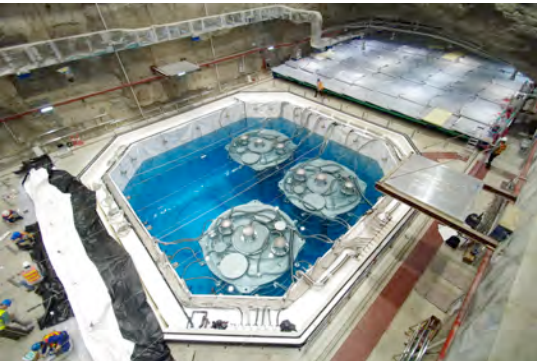
# Daya Bay Experiment Layout



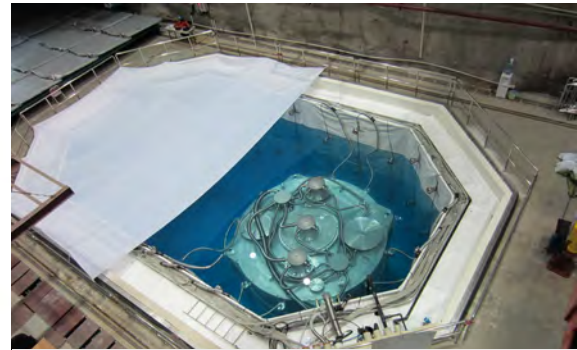
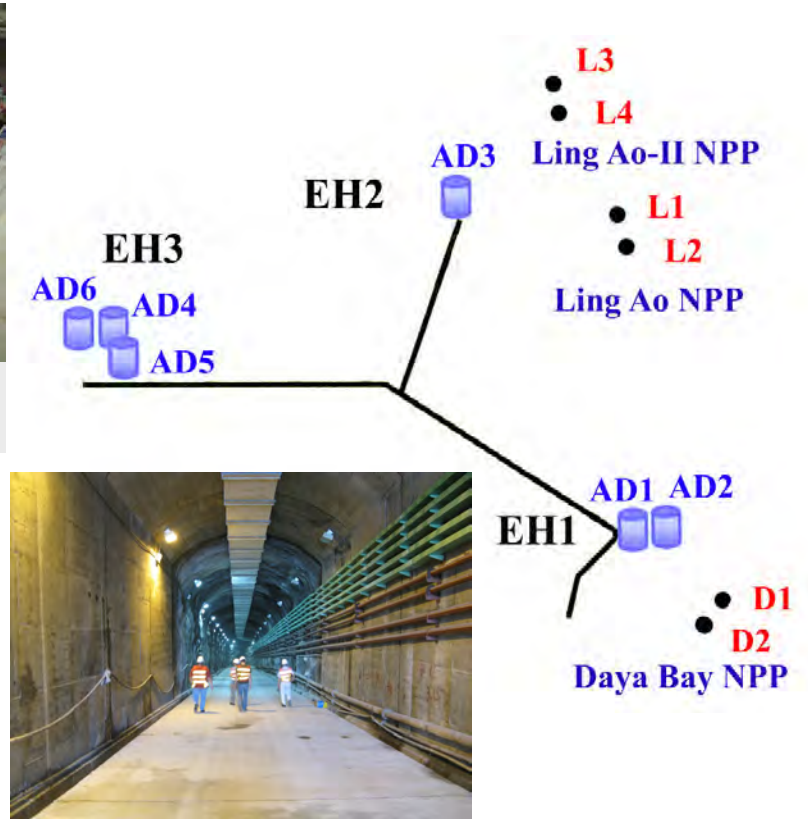
6 reactor cores  
 3 experimental halls  
 6 (8) detectors

	Overburden	$R_{\mu}$	$E_{\mu}$	D1,2	L1,2	L3,4
EH1	250	1.27	57	364	857	1307
EH2	265	0.95	58	1348	480	528
EH3	860	0.056	137	1912	1540	1548

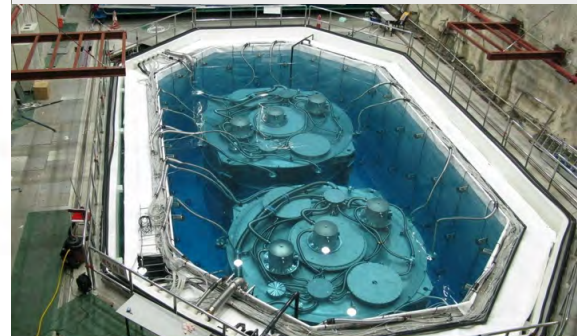
# Daya Bay Experiment Layout



Hall 3: began 3 AD operation on Dec. 24, 2011



Hall 2: began 1 AD operation on Nov. 5, 2011

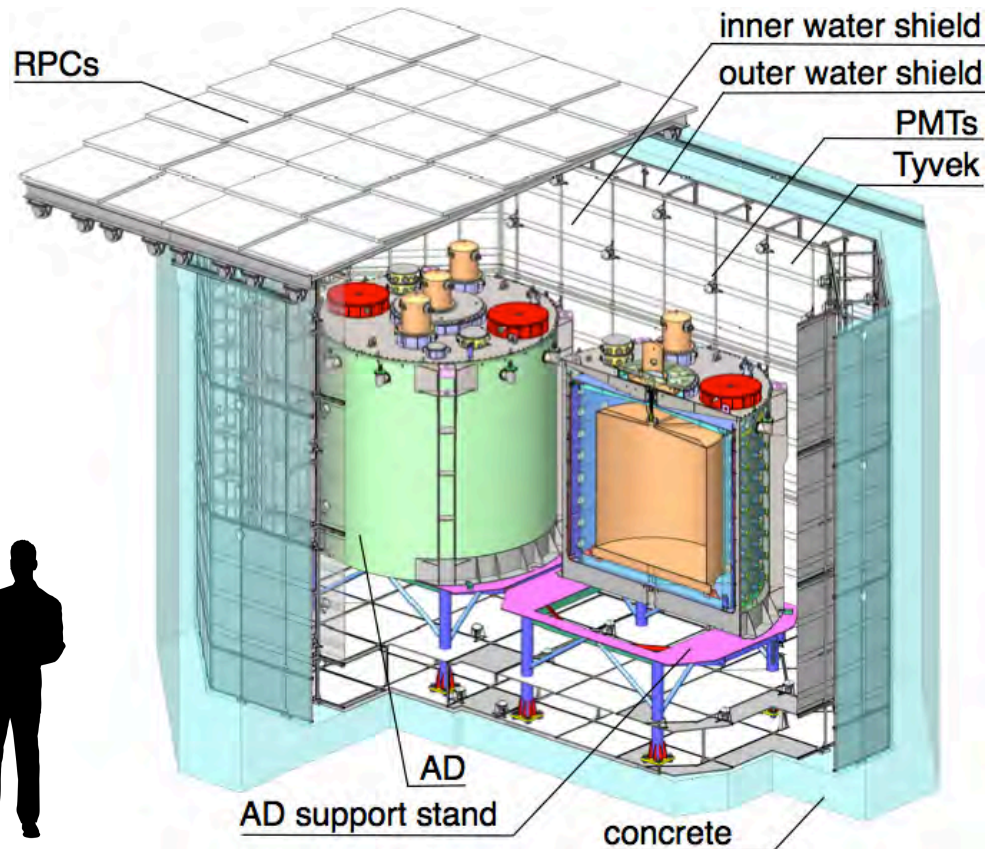
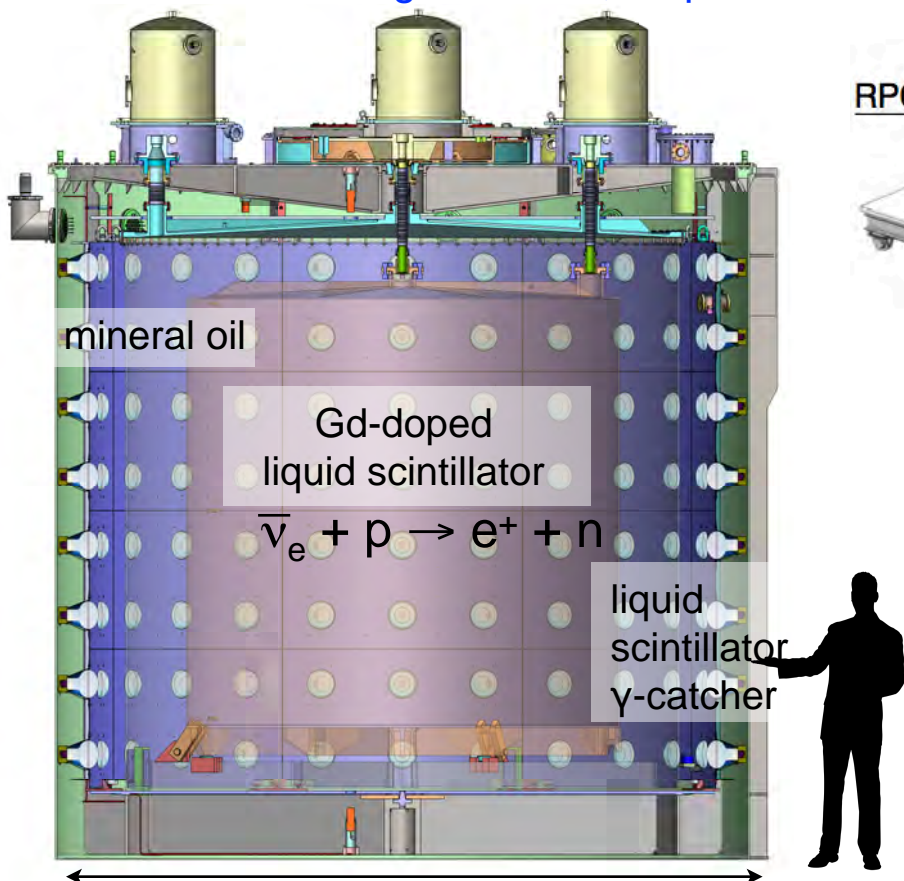


Hall 1: began 2 AD operation on Sep. 23, 2011

# Daya Bay Detectors

6 “functionally identical” detectors  
 Gd-LS defines target volume, no position cut

Dual tagging systems: 2.5 meter water shield and RPCs

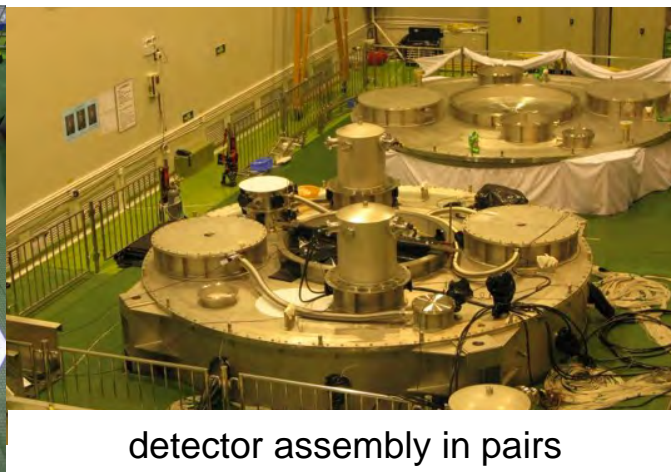
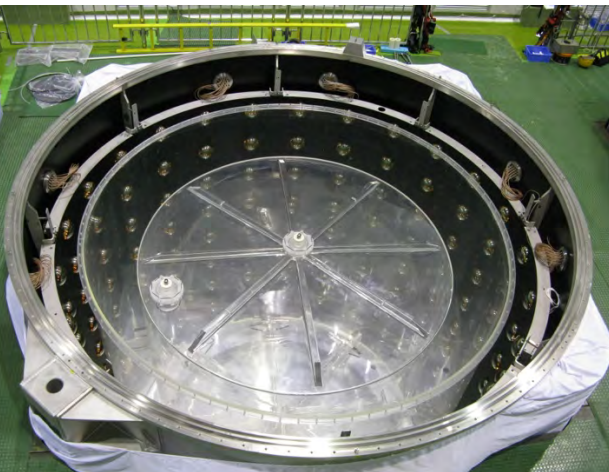
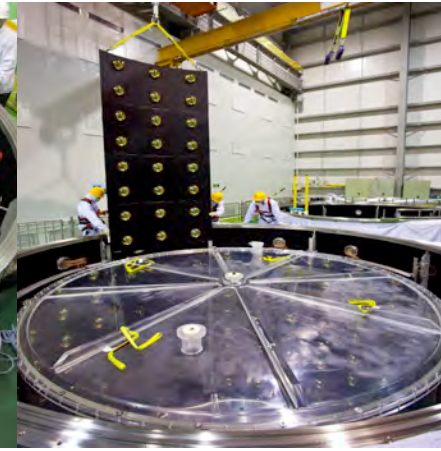
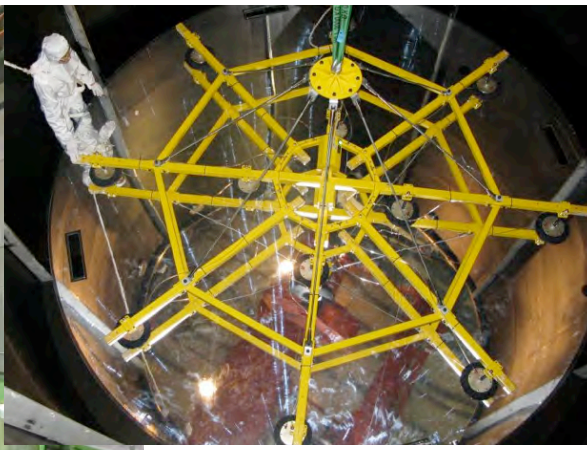
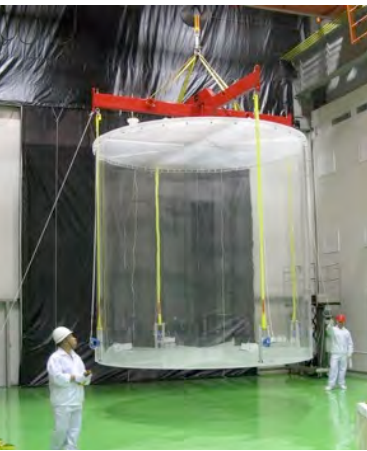
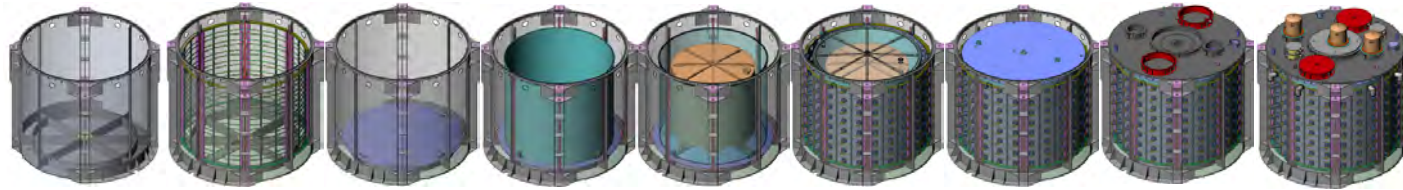


5 m  
 target mass: 20 ton per AD  
 photosensors: 192 8"-PMTs  
 energy resolution:  $(7.5 / \sqrt{E} + 0.9)\%$

Two-zone ultrapure water Cherenkov detector  
 multiple detectors allow comparison  
 and cross-checks



# Antineutrino Detector Assembly

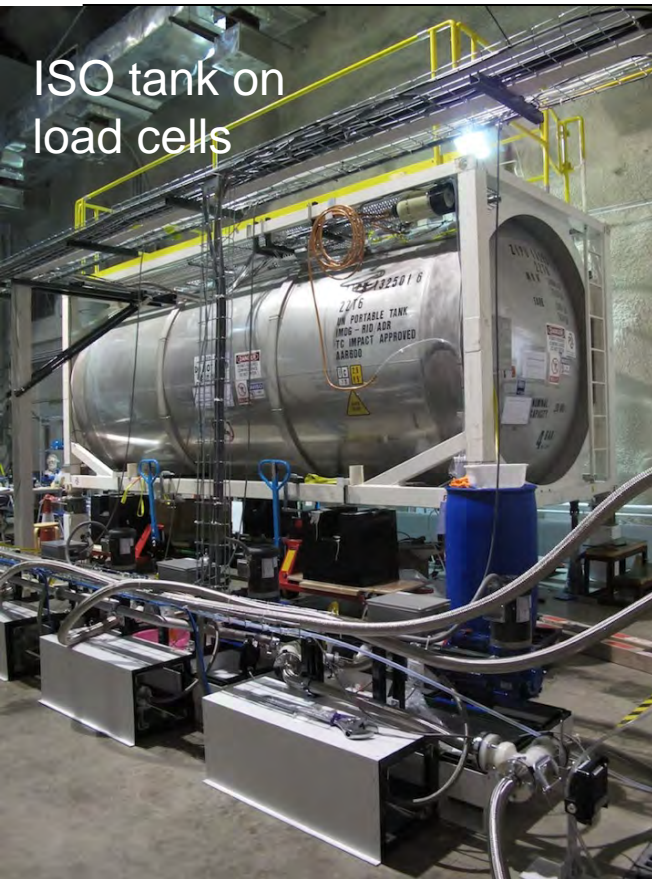


detector assembly in pairs

# Liquid Scintillator Hall



# Detector Filling and Target Mass Measurement

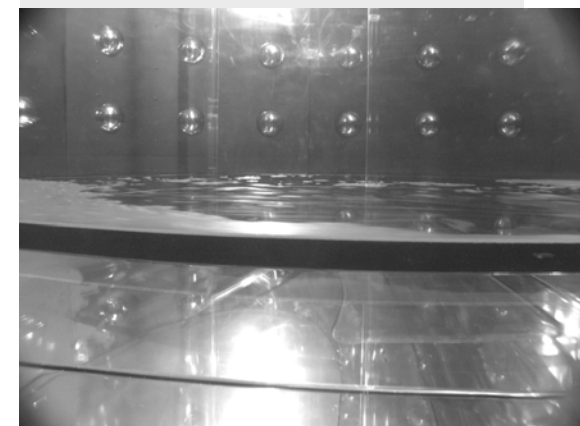
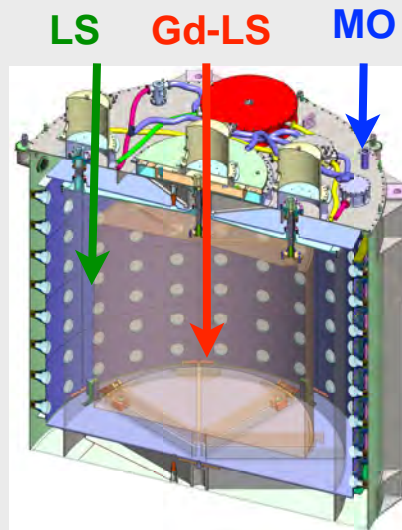


ISO tank on load cells



detector in scintillator hall

coriolis flow meters



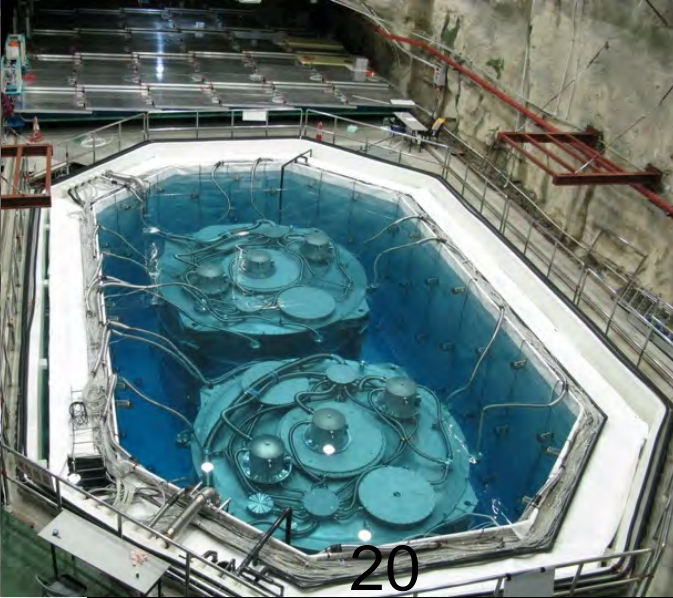
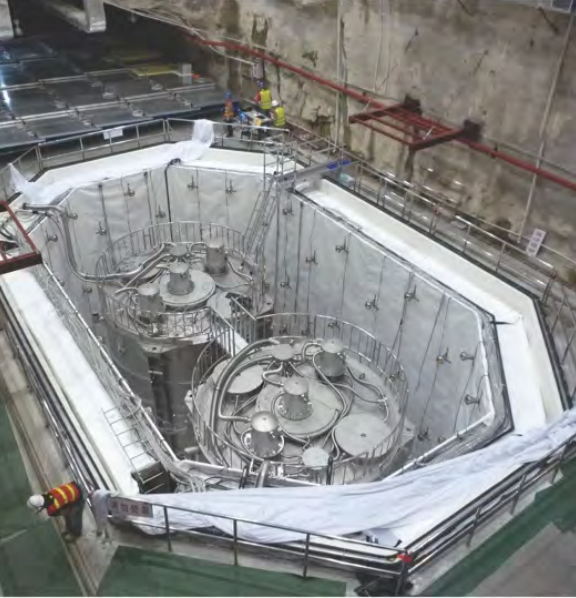
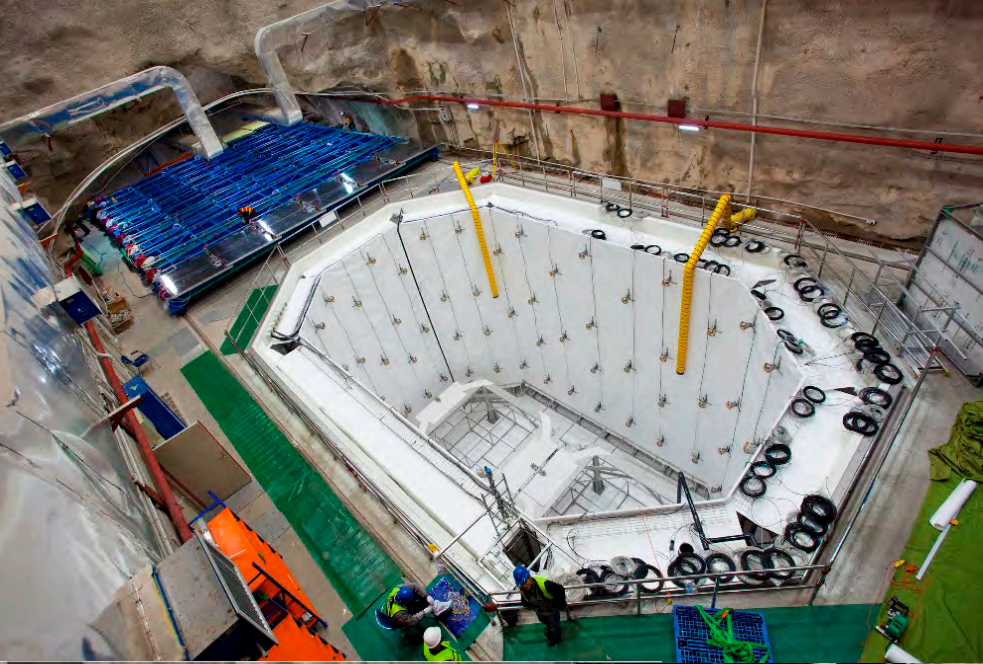
Detectors are filled from same reservoirs “in-pairs” within < 2 weeks.

Quantity	Relative	Absolute
protons/kg	neg.	0.47%
Density (kg/L)	neg.	neg.
Total mass	0.015%	0.015%
Overflow tank geometry	0.0066%	0.0066%
Overflow sensor calibration	0.0043%	0.0043%
Bellows Capacity	0.0025%	0.0025%
Target mass	0.017%	0.017%
Target protons	0.017%	0.47%

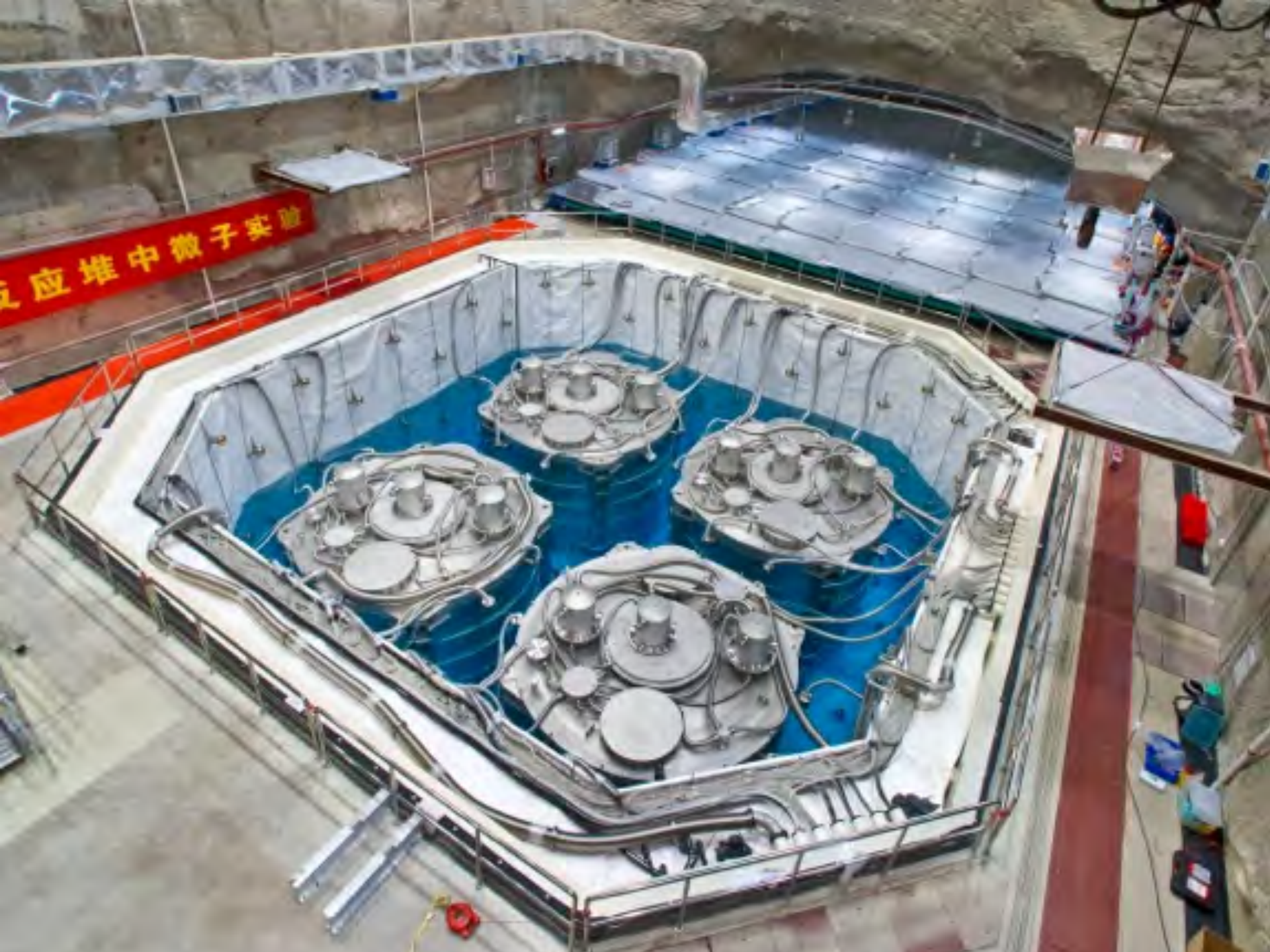
Target mass determination error  $\pm 3\text{kg}$  out of 20,000

<0.03% during data taking period

# Antineutrino Detector Installation - Near Hall

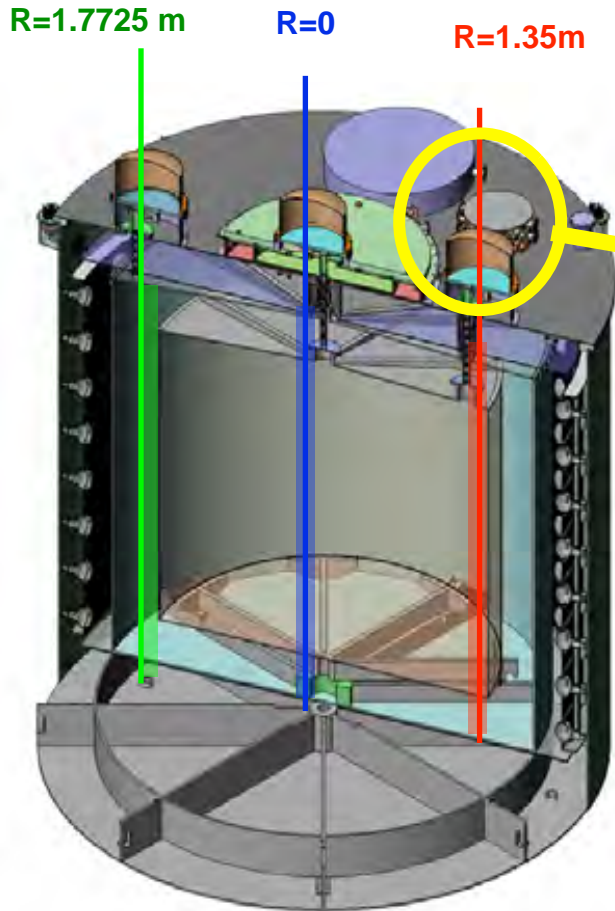


反应堆中微子实验

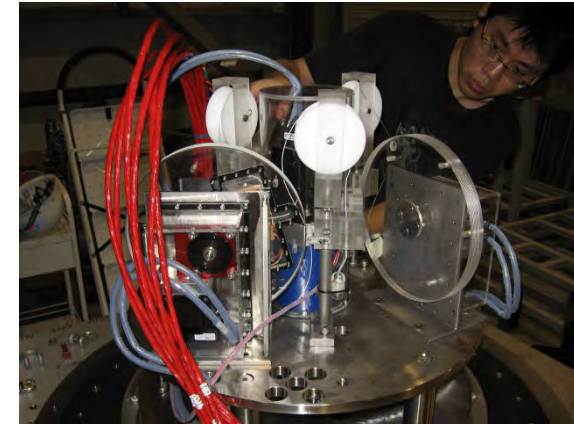
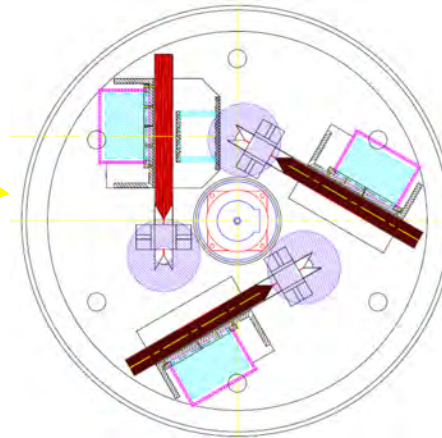


# Automated Calibration System

3 Automatic calibration 'robots' (ACUs) on each detector



Top view



## 3 sources in each robot, including:

- 10 Hz  $^{68}\text{Ge}$  (0 KE  $e^+$  =  $2 \times 0.511$  MeV  $\gamma$ 's)
- 0.75 Hz  $^{241}\text{Am}$ - $^{13}\text{C}$  neutron source (3.5 MeV n without  $\gamma$ )  
+ 100 Hz  $^{60}\text{Co}$  gamma source (1.173+1.332 MeV  $\gamma$ )
- LED diffuser ball (500 Hz) for time calibration

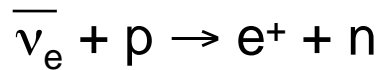
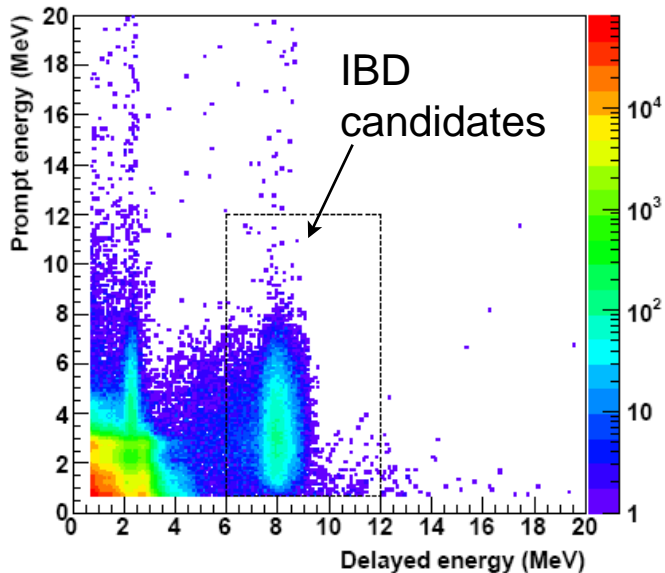
## Temporary special calibration sources:

- $\gamma$ :  $^{137}\text{Cs}$  (0.662 MeV),  $^{54}\text{Mn}$  (0.835 MeV),  $^{40}\text{K}$  (1.461 MeV)  
n:  $^{241}\text{Am}$ - $^9\text{Be}$ ,  $^{239}\text{Pu}$ - $^{13}\text{C}$

Three axes: center, edge of target, middle of gamma catcher

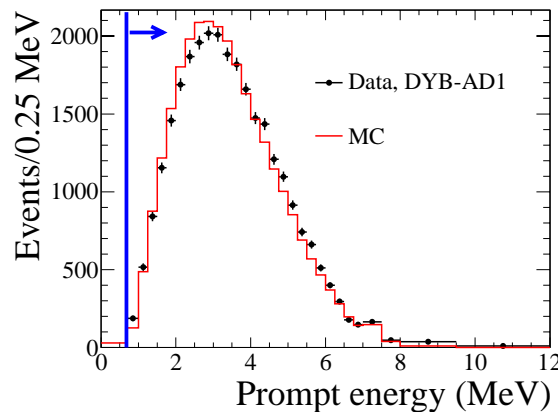
# Antineutrino Candidates (Inverse Beta Decay)

## Prompt + Delayed Selection

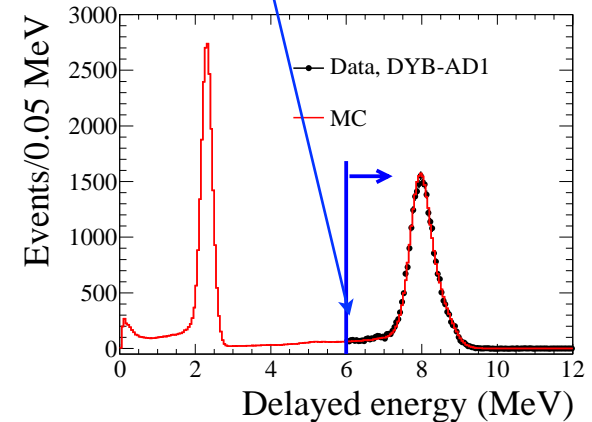


Uncertainty in relative  $E_d$  efficiency (0.12%)  
between detectors is largest systematic.

### Prompt Energy Signal



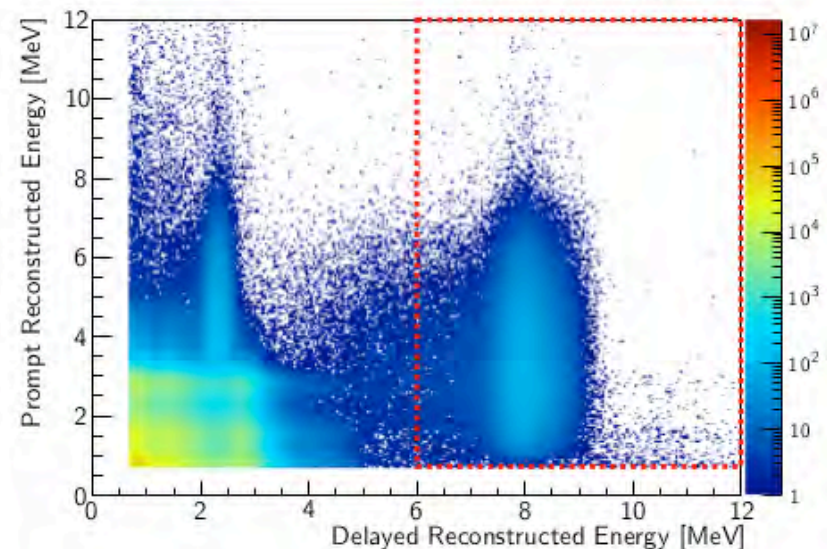
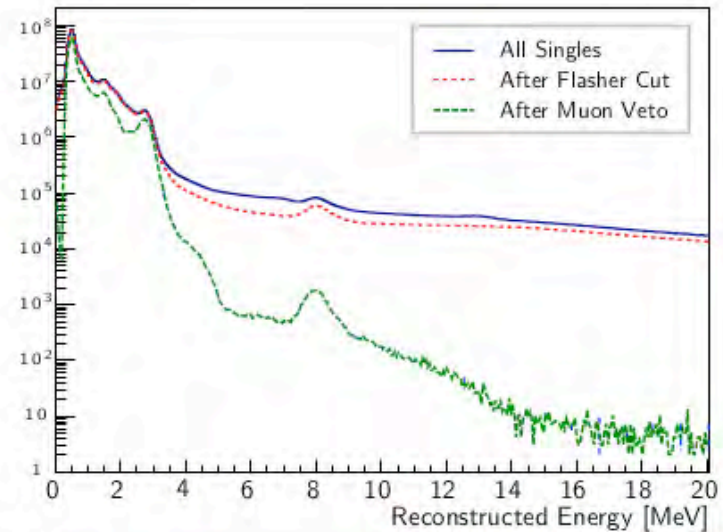
### Delayed Energy Signal



# Antineutrino Candidates Selection

Antineutrino interactions cleanly separated from backgrounds

- (1) Reject spontaneous PMT light emission ("flashers")
- (2) Prompt positron:  
 $0.7 \text{ MeV} < E_p < 12 \text{ MeV}$
- (3) Delayed neutron:  
 $6.0 \text{ MeV} < E_d < 12 \text{ MeV}$
- (4) Neutron capture time:  
 $1 \mu\text{s} < t < 200 \mu\text{s}$
- (5) Muon veto:
  - Water pool muon (>12 hit PMTs):  
Reject [-2 $\mu\text{s}$ ; 600 $\mu\text{s}$ ]
  - AD muon (>3000 photoelectrons):  
Reject [-2  $\mu\text{s}$ ; 1400 $\mu\text{s}$ ]
  - AD shower muon (> $3 \times 10^5$  p.e.):  
Reject [-2  $\mu\text{s}$ ; 0.4s]
- (6) Multiplicity:
  - No additional prompt-like signal  
400 $\mu\text{s}$  before delayed neutron
  - No additional delayed-like signal  
200 $\mu\text{s}$  after delayed neutron





# Analyzed Data Sets

## Two detector comparison

[1202.6181]

- 90 days of data, Daya Bay near only
- NIM A **685** (2012), 78-97

## First oscillation analysis

[1203:1669]

- 55 days of data, 6 ADs near+far
- PRL **108** (2012), 171803

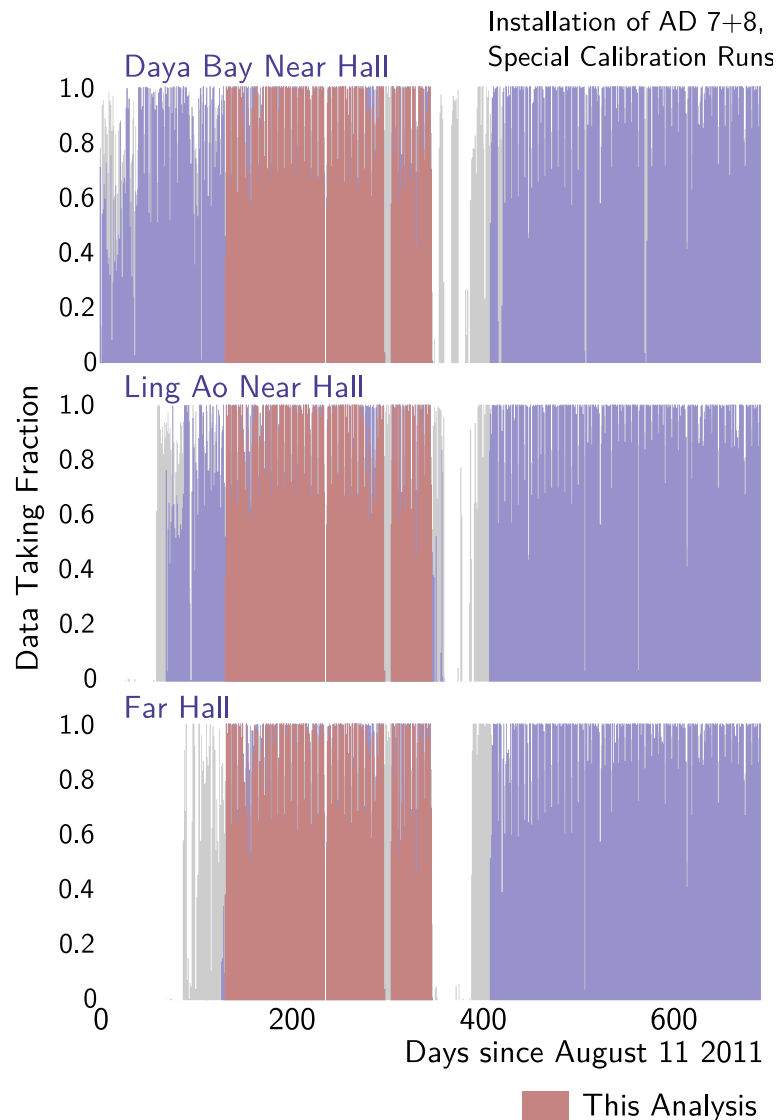
## Improved oscillation analysis

[1210.6327]

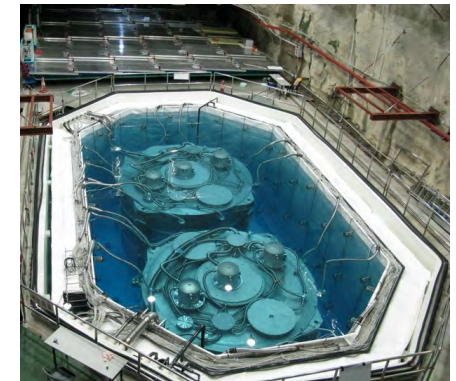
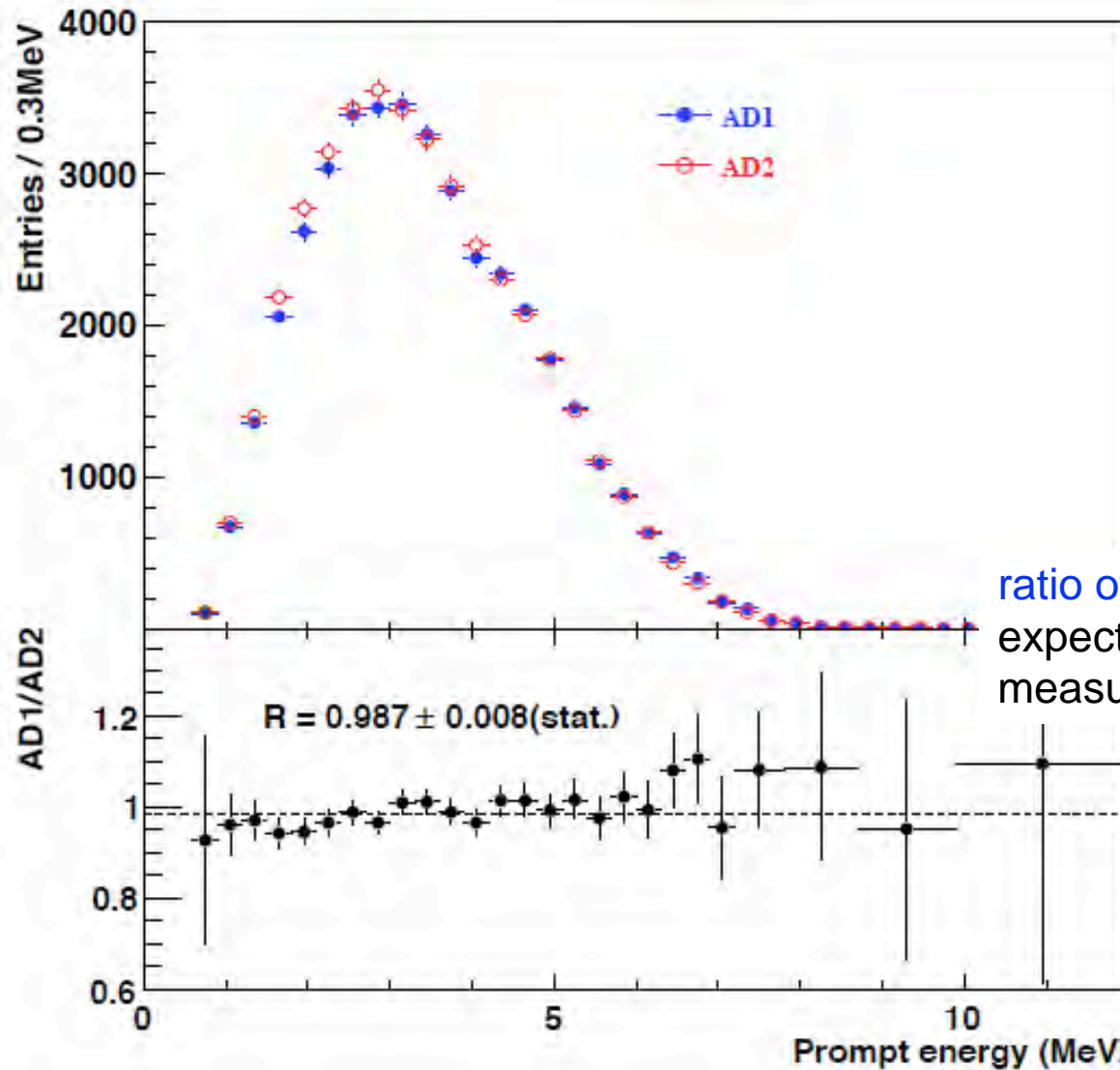
- 139 days of data, 6 ADs near+far
- CP C **37** (2013), 011001

## Spectral Analysis

- 217 days complete 6 AD period
- 55% more statistics than CPC result



# Side-by-Side Comparison in Near Hall



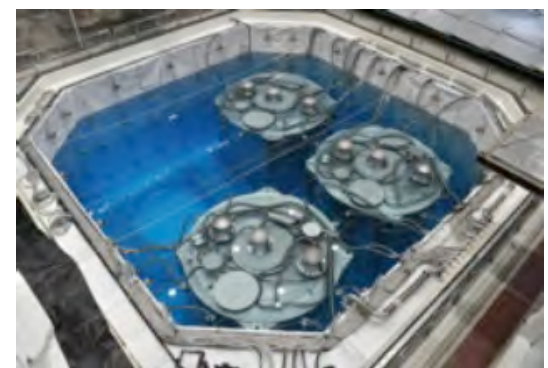
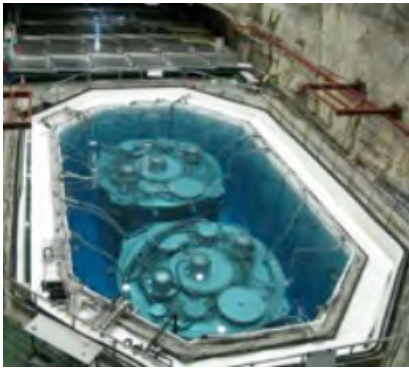
Feb 2012

ratio of neutrino events in AD1 and AD2  
expected: 0.981  
measured:  $0.987 \pm 0.008 \text{ (stat)} \pm 0.003$

ratio is not 1 because of  
baseline difference

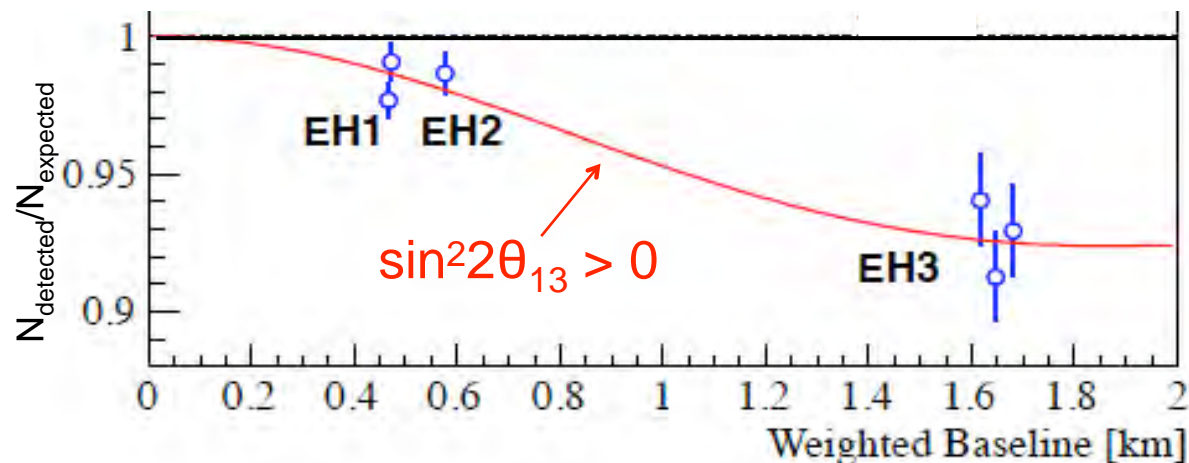
Daya Bay Collab. arXiv:1202:6181 (2012)

# Daya Bay Initial Results



March 2012

Based on 55 days of data with 6 ADs, discovered disappearance of reactor  $\bar{\nu}_e$  at short baseline. [PRL 108, 171803]



June 2012

Obtained the most precise value of  $\theta_{13}$ :

$$\sin^2 2\theta_{13} = 0.089 \pm 0.010 \pm 0.005 \quad [\text{CPC } 37, 011001]$$

TALENs, and another genome-editing tool called meganucleases is that they must be reengineered for each new DNA target. These proteins have two parts: the DNA targeting section and the DNA-cutting section. The new technology substitutes RNA—which is simpler to make than a piece of a protein—for the DNA targeting section. It also makes

use of a bacterial protein called Cas9, which is part of a natural bacterial defense system called CRISPR, to do the cutting.

Researchers have shown in a test-tube that they can combine these two RNAs into a single one that both matches the DNA target and holds Cas9 in place. Using this system, they were able to cut specific target DNA,

demonstrating the potential of Cas9 to work like TALENs. Now, those researchers are trying this approach in organisms other than bacteria, and other genome engineers are quite excited about their prospects, suggesting that it may one day challenge zinc finger nucleases and TALENs as the core genome engineering technology.

## CRASH PROJECT OPENS A DOOR IN NEUTRINO PHYSICS

Sometimes it's not the result itself so much as the promise it holds that matters most. This year, physicists measured the last parameter describing how elusive particles called neutrinos morph into one another as they zip along at near-light speed. And the result suggests that in the coming decades neutrino physics will be every bit as rich as physicists had hoped—and may even help explain how the universe evolved to contain so much matter and so little antimatter.

Born in certain nuclear interactions, neutrinos come in three types or flavors that change into one another in so-called neutrino oscillations. The rates and extents to which the flavors mix depend on six parameters: the three differences between the neutrinos' masses, and three "mixing angles." In March, the 250 researchers with the Daya Bay Reactor Neutrino Experiment in China reported that last unknown parameter, the mixing angle known as  $\theta_{13}$  (pronounced "theta one three"), equals  $8.8^\circ$ , give or take  $0.8^\circ$ .

The result itself is remarkable, as it's not every year that physicists measure a new fundamental parameter. The real excitement, however, stems from the result's broader implications. The measurement proves that all three mixing angles are greater than zero. That fact, in turn, implies that the oscillations of antineutrinos might differ from those of neutrinos, something that would not be possible had  $\theta_{13}$  equaled zero.

That's a big deal. Such a difference would

be analogous to the effect that created the matter-antimatter imbalance in the universe.

In fact, researchers in the United States, Japan, and Europe are engaged in experiments in which they use particle accelerators to fire neutrinos hundreds of kilometers through Earth to huge particle detectors. Current efforts seek to pin down, for example,

the neutrinos emanating from the reactors at the Daya Bay Nuclear Power Plant and two neighboring plants in Shenzhen. In making a definitive measurement, they beat out teams working at reactors in France and South Korea and accelerator-based experiments in Japan and the United States.

The measurement of  $\theta_{13}$  wasn't the only result in particle physics this year. Researchers working with the world's largest atom smasher, the Large Hadron Collider (LHC) in Switzerland, discovered the Higgs boson, the

2/AF IMAGES



That was fast! Construction of China's Daya Bay Reactor Neutrino Experiment began in 2007. With 2 months' worth of data, it scooped competitors in Japan, France, Korea, and the United States.

Science 338, 1527

## Rate-only Analysis:

*Previously reported*

$$\frac{N_{far}}{N_{near}} = \frac{N_{protons, far}}{N_{protons, near}} \frac{L_{near}^2}{L_{far}^2} \frac{\epsilon_{far}}{\epsilon_{near}} \frac{\int_{E_{min}}^{E_{max}} dE P_{surv}(E, L_{far}; \theta_{13}, \Delta m_{ee}^2) \sigma(E) \Phi(E)}{\int_{E_{min}}^{E_{max}} dE P_{surv}(E, L_{near}; \theta_{13}, \Delta m_{ee}^2) \sigma(E) \Phi(E)}$$

**Advantages:** Fewer systematic uncertainties

**Disadvantages:** Less sensitive, Unable to constrain  $\Delta m_{ee}^2$

## Rate + Spectrum Analysis:

*Latest result*

$$\frac{\frac{dN_{far}}{dE}}{\frac{dN_{near}}{dE}} = \frac{N_{protons, far}}{N_{protons, near}} \frac{L_{near}^2}{L_{far}^2} \frac{\epsilon_{far}}{\epsilon_{near}} \frac{P_{surv}(E, L_{far}; \theta_{13}, \Delta m_{ee}^2) \sigma(E) \Phi(E)}{P_{surv}(E, L_{near}; \theta_{13}, \Delta m_{ee}^2) \sigma(E) \Phi(E)}$$

**Advantages:** Each energy bin is an independent oscillation measurement,  $\Delta m_{ee}^2$

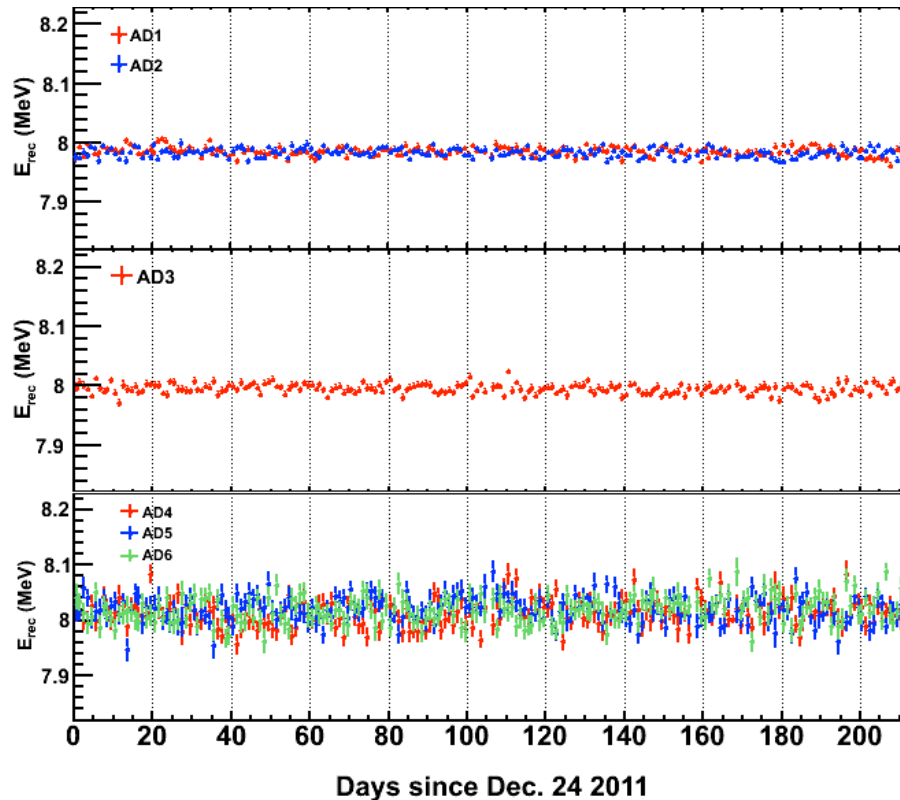
**Disadvantages:** Requires detailed understanding of detector energy response.

# Calibration Performance

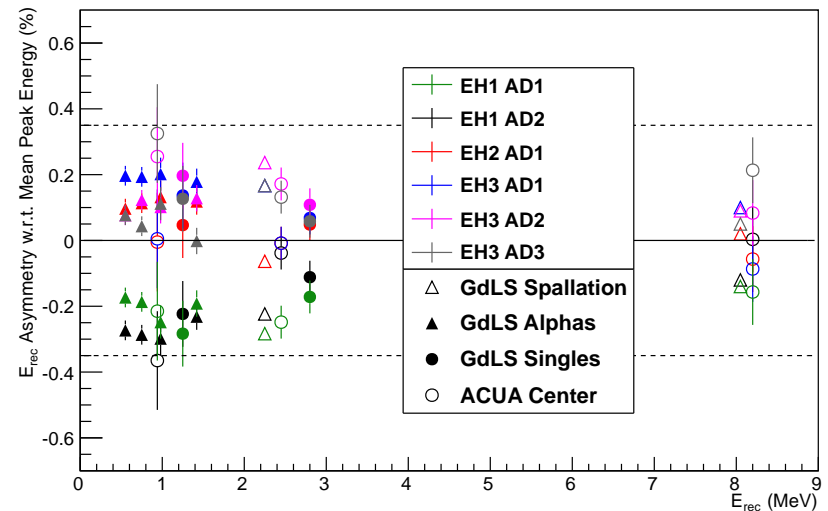
## Stable and Consistent Energy Response

After calibration, achieve energy response that is **stable to ~0.1%** in all detectors, with a **total relative uncertainty of 0.35%** between detectors.

### Spallation $n$ Gd capture peak vs. time (after all calibration)



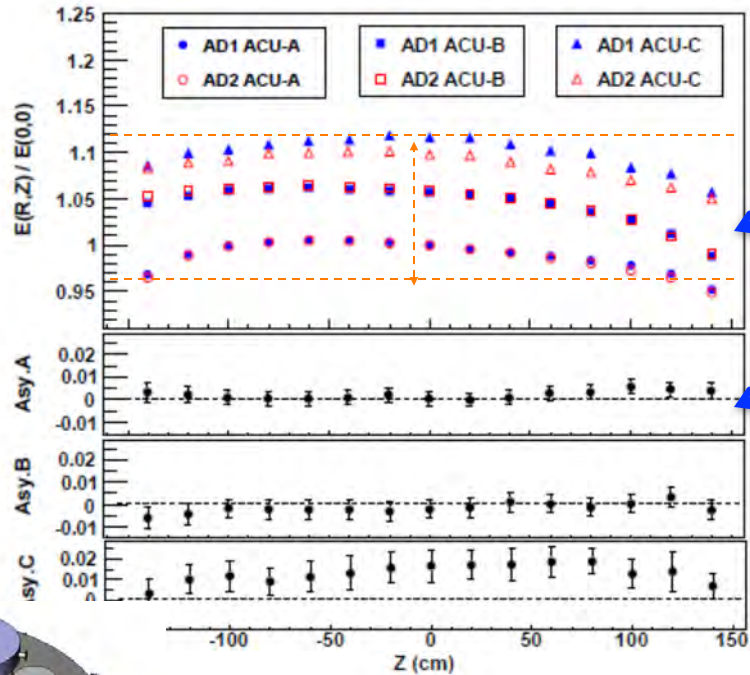
### Relative energy peaks in all detectors (after calibration)



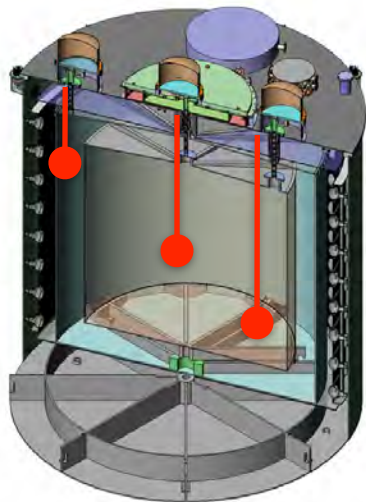
# Calibration: Detector Uniformity

Measure uniformity with sources placed along three axes and spallation nGd events

Example:  $^{60}\text{Co}$

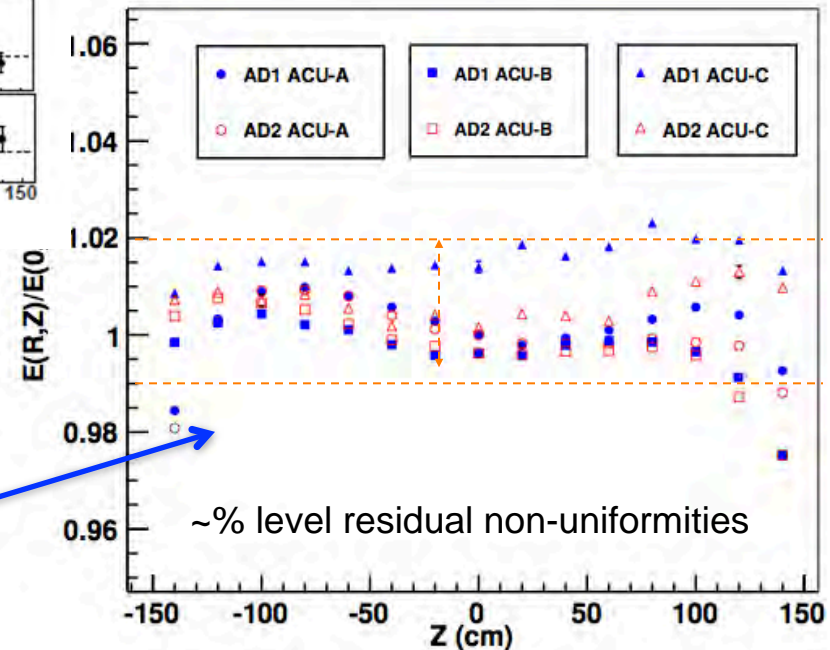


Energy response varies across detector...  
...but still consistent between detectors



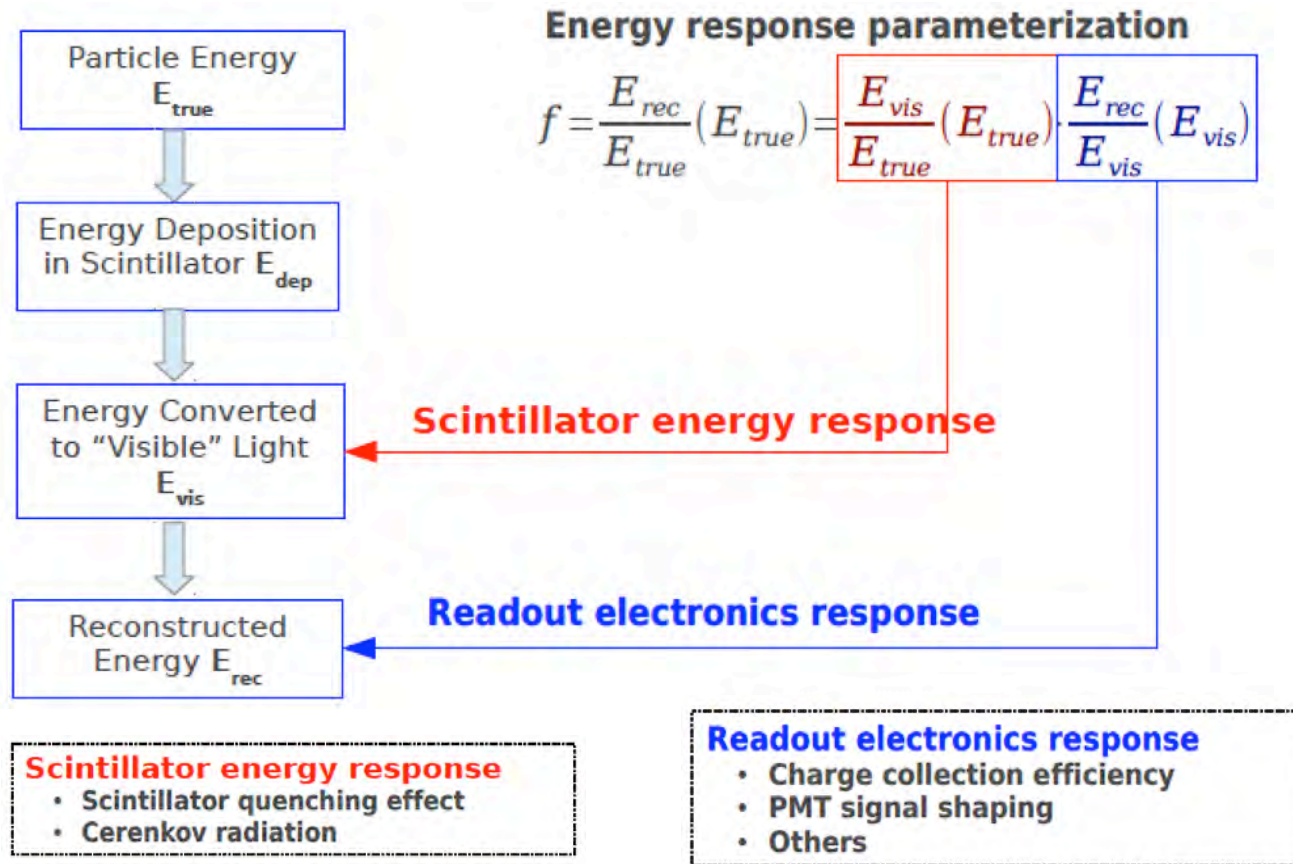
3 sources along 3 axes

After first-order correction, energy is more uniform.



# Energy Response Model

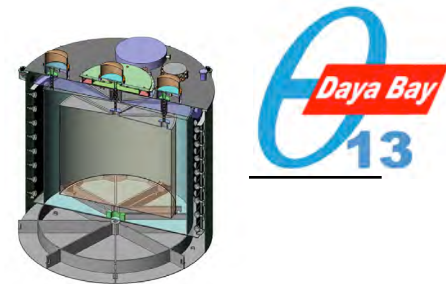
Model maps true energy  $E_{true}$  to reconstructed kinetic energy  $E_{rec}$



- Minimal impact on oscillation measurement
- Crucial for measurement of reactor spectra



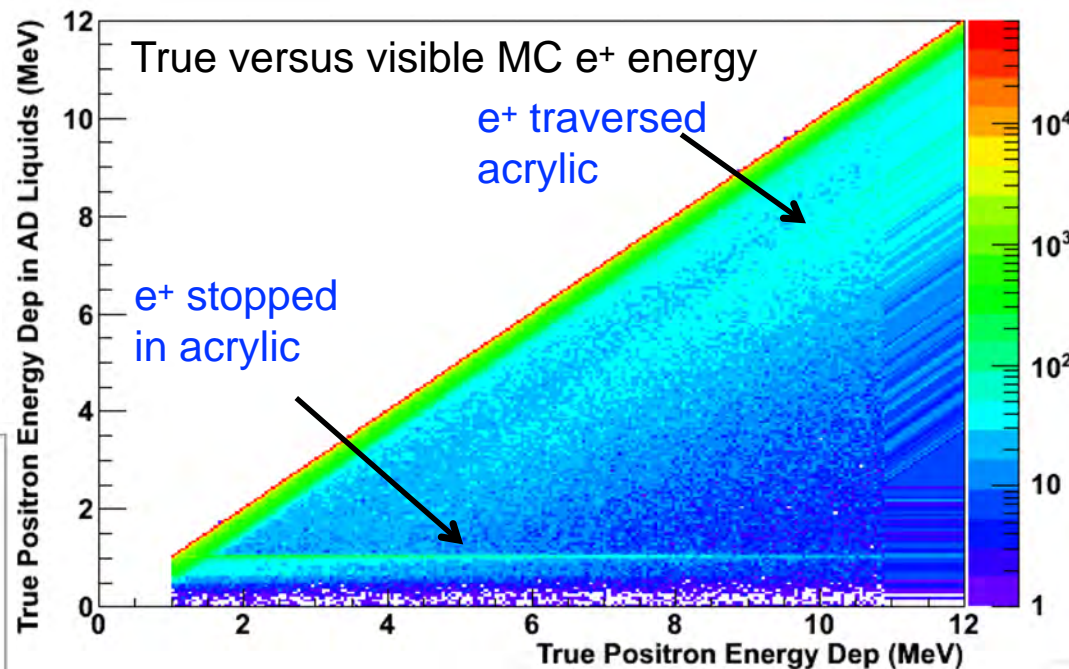
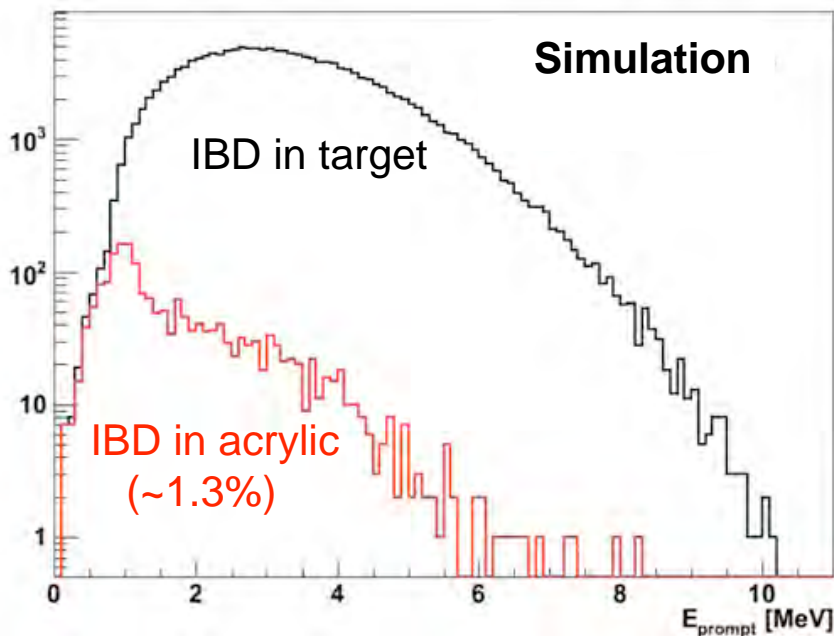
# Detector Response: Acrylic Vessels



Energy loss in acrylic causes small distortion of energy spectrum

If antineutrino interacts in or near acrylic vessel, a portion of the kinetic energy of inverse beta positrons will not be detected

Annihilation gammas with longer range can also deposit energy in the vessels



**Generated 2D distortion matrix from MC to correct predicted positron energy spectrum**

Uncertainties from varying acrylic vessel thicknesses and MC statistics incorporated into analysis.

# Scintillator Response Model

## Electron response

2 parameterizations to model quenching effects and Cherenkov radiation:

1) 3-parameter purely empirical model:

$$\frac{E_{\text{vis}}}{E_{\text{true}}} = \frac{1 + p_3 \cdot E_{\text{true}}}{1 + p_1 \cdot e^{-p_2 \cdot E_{\text{true}}}}$$

2) Semi-emp. model based on Birks' law:

$$\frac{E_{\text{vis}}}{E_{\text{true}}} = f_q(E_{\text{true}}; k_B) + k_C \cdot f_c(E_{\text{true}})$$

$k_B$ : Birks' constant  
 $k_C$ : Cherenkov contribution

## Gammas + positrons

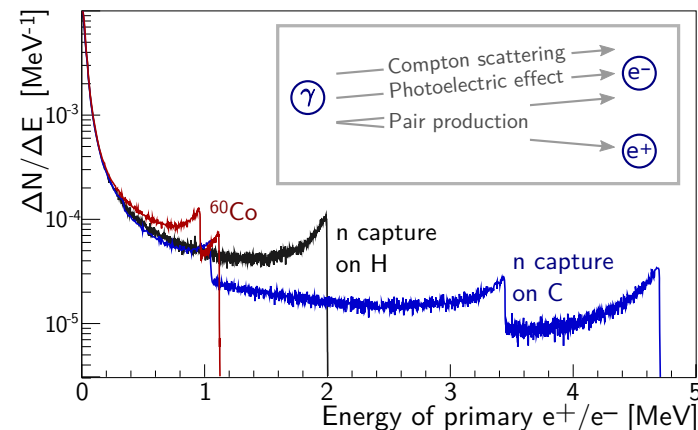
- Gammas connected to electron model through MC:

$$E_{\text{vis}}^{\gamma} = \int E_{\text{vis}}^{e^-}(E_{\text{true}}) \cdot \frac{dN}{dE}(E_{\text{true}}) dE_{\text{true}}^{e^-}$$

- Positrons connected to electron model through MC:

$$E_{\text{vis}}^{e^+} = E_{\text{vis}}^{e^-} + 2 \cdot E_{\text{vis}}^{\gamma}(0.511 \text{ MeV})$$

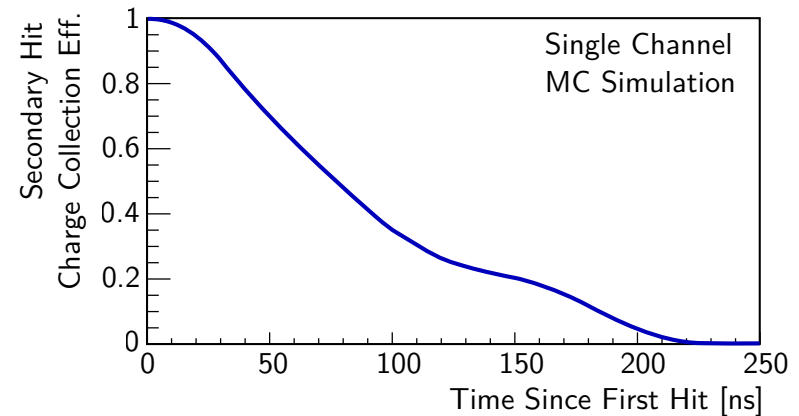
Simulation of individual  $e^-$ ,  $e^+$  energies due to gamma interaction in scintillator.



## PMT readout electronics introduces additional biases

Electronics does not fully capture late secondary hits

- Slow scintillation component missed at high energies
- Charge collection efficiency decreases with visible light



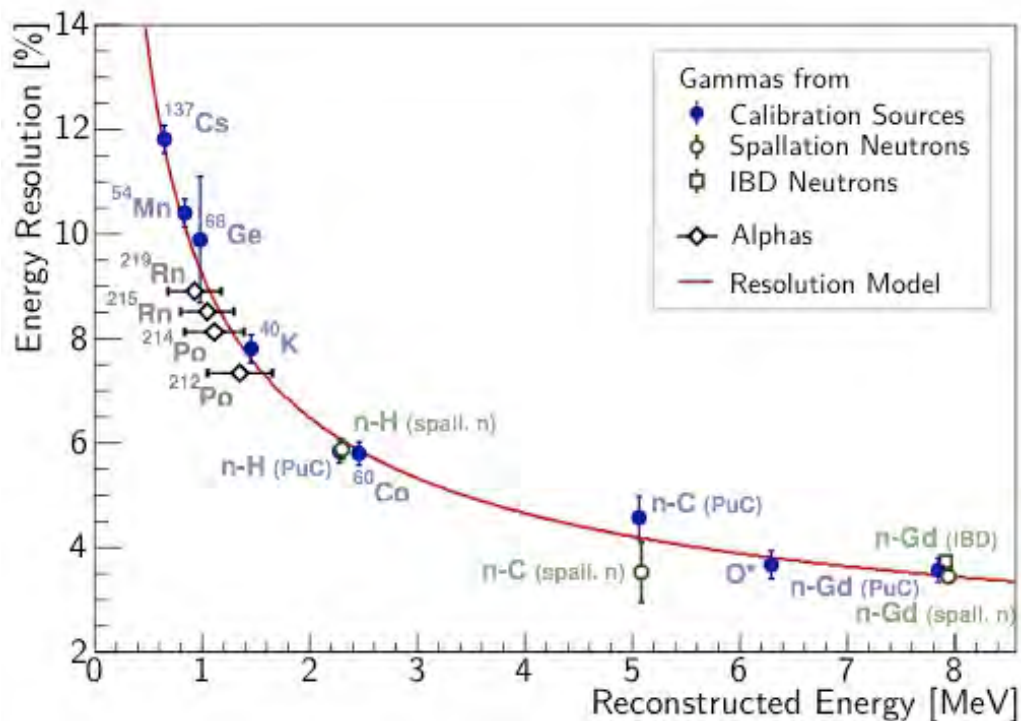
## PMT readout electronics introduces additional biases

- Effective model as a function of total visible energy
- 2 empirical parameterizations: exponential and quadratic
- Total effective non-linearity  $f$  from both scintillation and electronics effects:

$$f = \frac{E_{\text{rec}}}{E_{\text{true}}} = \frac{E_{\text{rec}}}{E_{\text{vis}}} \cdot \frac{E_{\text{vis}}}{E_{\text{true}}}$$

- 1 Electronics non-linearity
- 2 Scintillator non-linearity

# Energy Resolution Model



Functional form:

$$\frac{\sigma_E}{E} = \sqrt{a^2 + \frac{b^2}{E} + \frac{c^2}{E^2}}$$

Contributions from:

- a : Spacial/temp. resolution ( $\propto E$ )
- b : Photon statistics ( $\propto \sqrt{E}$ )
- c : Dark noise (const:)

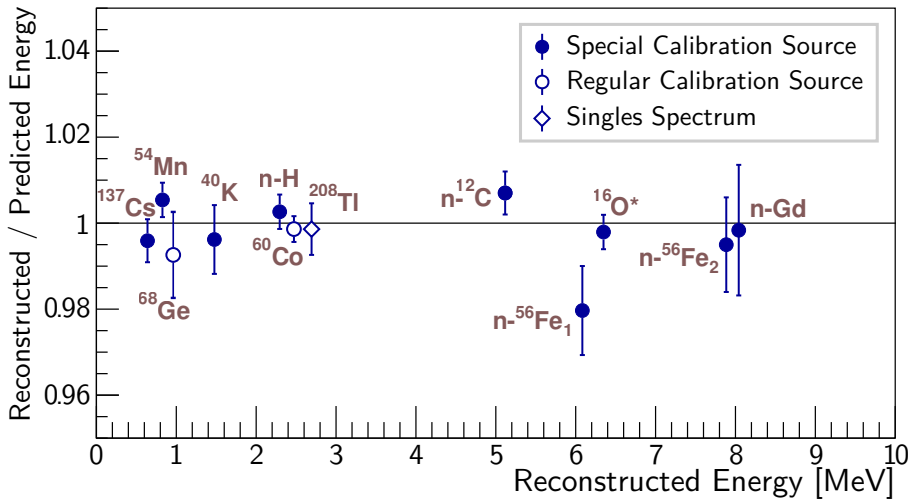
Calibrated primarily using monoenergetic gamma sources

- Radioactive calibration sources placed at the detector center
- Additional data from IBD and spallation neutrons, uniformly distributed in LS
- Alpha source data used to cross-check result
  - Larger uncertainties due to different response from electronics

# Constraining the Non-Linearity Parameters

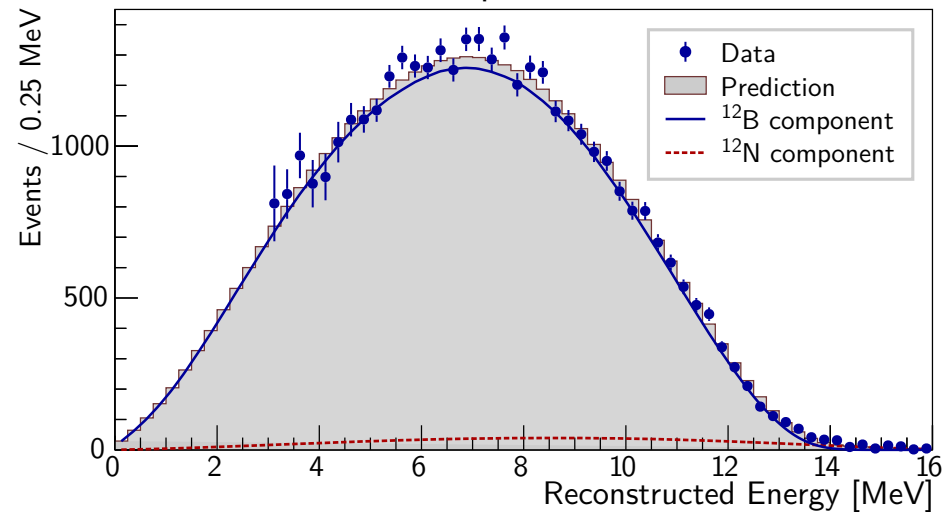
## Gamma Ray Energy Peaks

Gamma Sources



## $^{12}\text{B}$ Beta-Decay Spectrum

Boron Spectrum



### Full detector calibration data

#### 1. Monoenergetic gamma lines from various sources

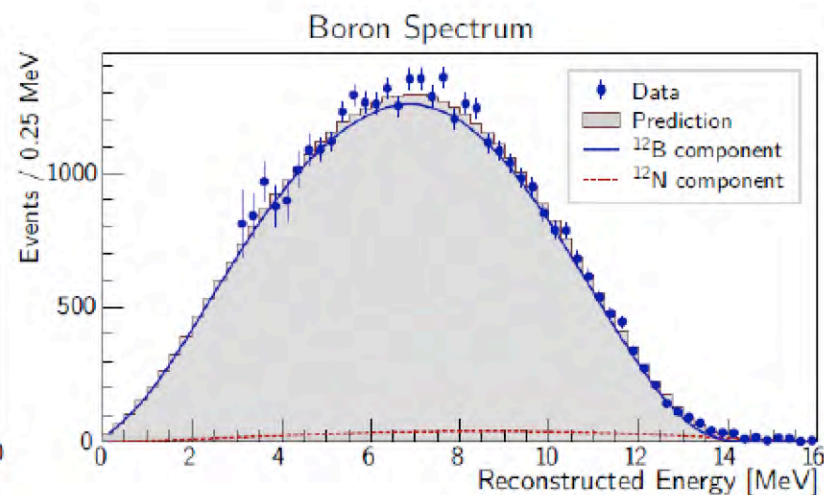
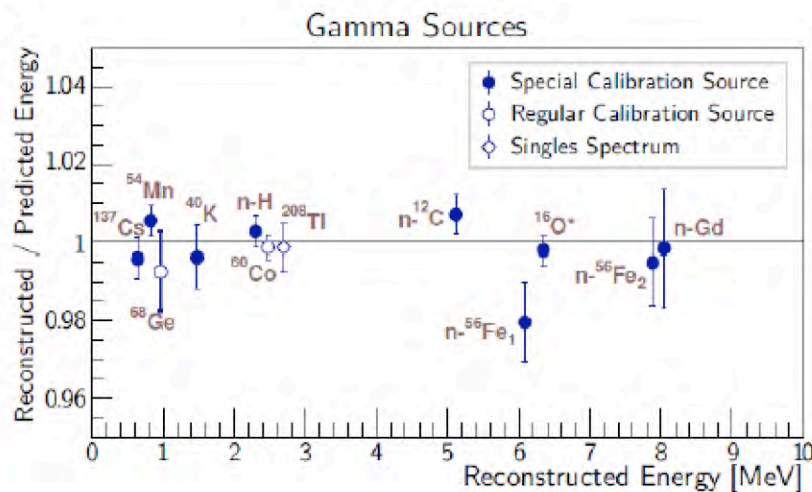
- Radioactive calibration sources, employed regularly:  $^{68}\text{Ge}$ ,  $^{60}\text{Co}$ ,  $^{241}\text{Am}$ - $^{13}\text{C}$  and during special calibration periods:  $^{137}\text{Cs}$ ,  $^{54}\text{Mn}$ ,  $^{40}\text{K}$ ,  $^{241}\text{Am}$ - $^9\text{Be}$ ,  $\text{Pu}$ - $^{13}\text{C}$
- Singles and correlated spectra in regular physics runs ( $^{40}\text{K}$ ,  $^{208}\text{Tl}$ , n capture on H)

#### 2. Continuous spectrum from $^{12}\text{B}$ produced by muon spallation inside the scintillator

### Standalone measurements

- Scintillator quenching measurements using neutron beams and Compton  $e^-$
- Calibration of readout electronics with flash ADC

## Constraints

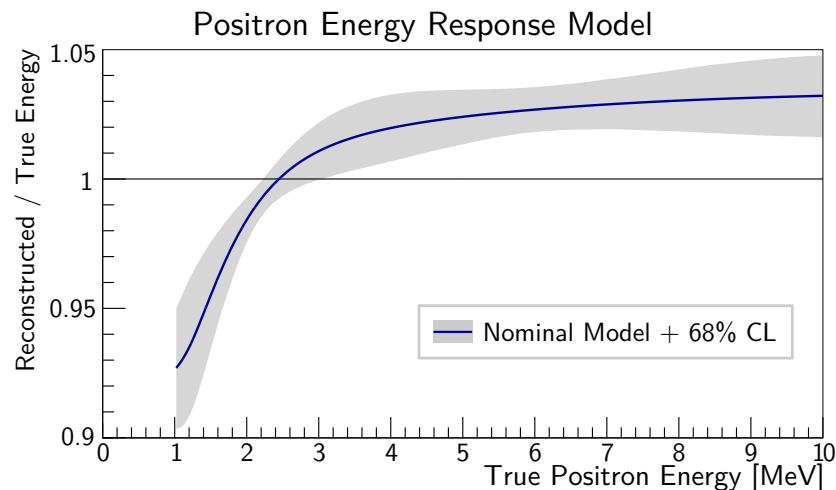


Use calibration gamma sources and continuous  $^{12}\text{B}$  spectrum to constrain energy model parameters

## Positron Energy Response

multiple models are constructed with different data and parameter constraints

conservatively combine 5 minimal correlated energy models



# Uncertainty Summary

	Detector		Uncorrelated
	Efficiency	Correlated	
Target Protons		0.47%	0.03%
Flasher cut	99.98%	0.01%	0.01%
Delayed energy cut	90.9%	0.6%	0.12%
Prompt energy cut	99.88%	0.10%	0.01%
Multiplicity cut		0.02%	<0.01%
Capture time cut	98.6%	0.12%	0.01%
Gd capture ratio	83.8%	0.8%	<0.1%
Spill-in	105.0%	1.5%	0.02%
Livetime	100.0%	0.002%	<0.01%
Combined	78.8%	1.9%	0.2%

For near/far oscillation, only uncorrelated uncertainties are used.

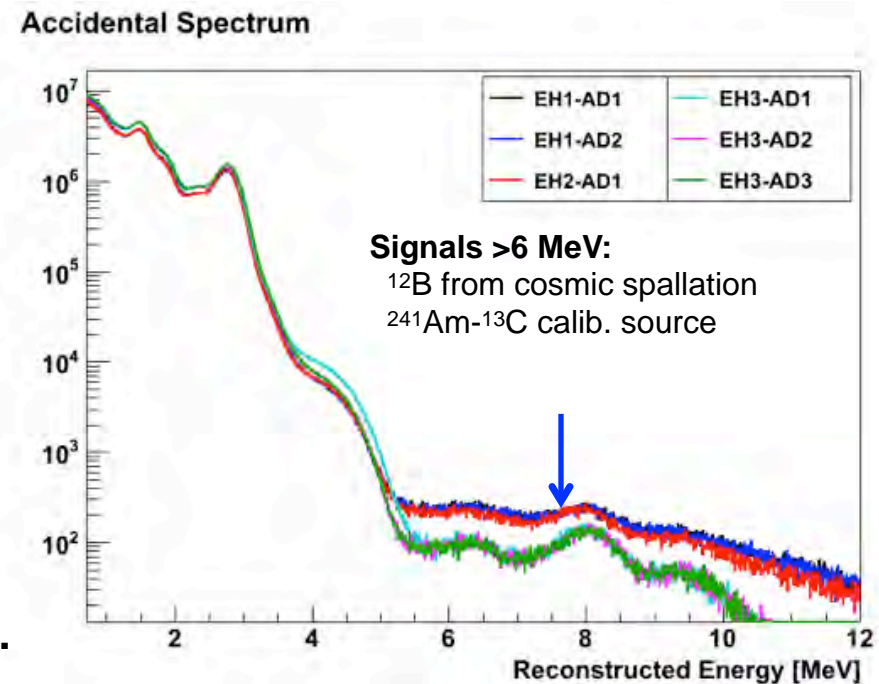
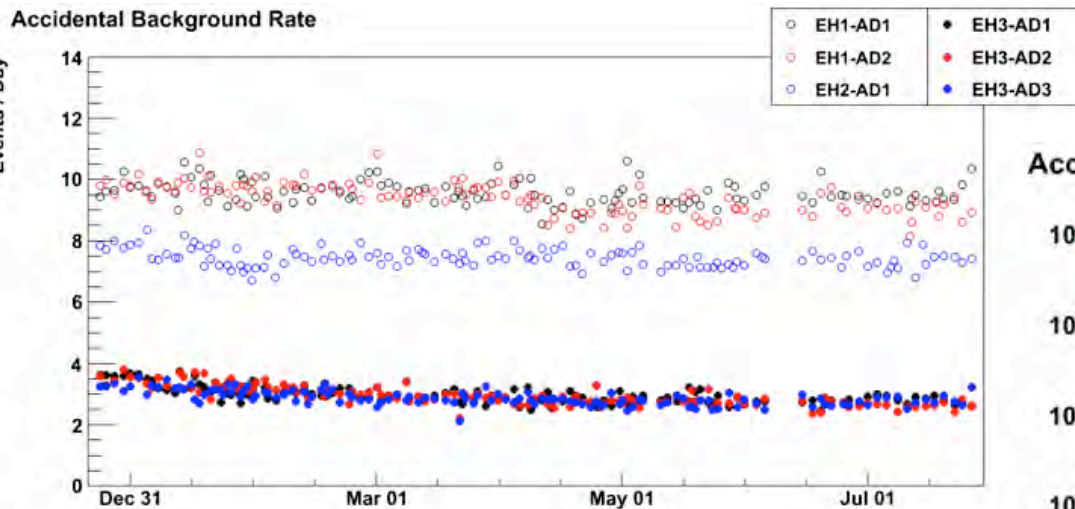
Largest systematics are smaller than far site statistics (~0.5%)

Reactor			
Correlated		Uncorrelated	
Energy/fission	0.2%	Power	0.5%
$\bar{\nu}_e$ /fission	3%	Fission fraction	0.6%
		Spent fuel	0.3%
Combined	3%	Combined	0.8%

Influence of uncorrelated reactor systematics reduced by far vs. near measurement.

# Accidental Background

Two uncorrelated signals can accidentally mimic an antineutrino signal.



Accidental B/S is 4% (1.5%) of far (near) signal.

Accidental background be accurately modeled using uncorrelated signals in data.

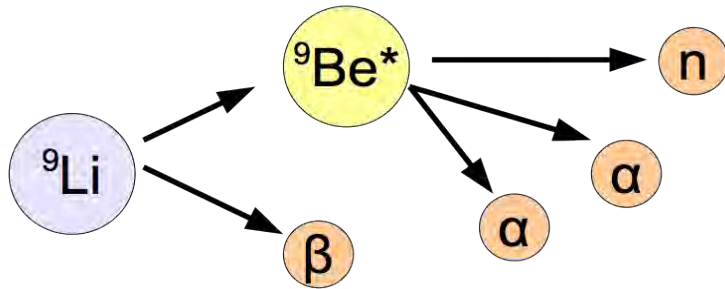
➔ Negligible uncertainty in background rate or spectra.



# Background: $\beta$ -n decay

## $\beta$ -n decay:

- Prompt:  $\beta$ -decay
- Delayed: neutron capture



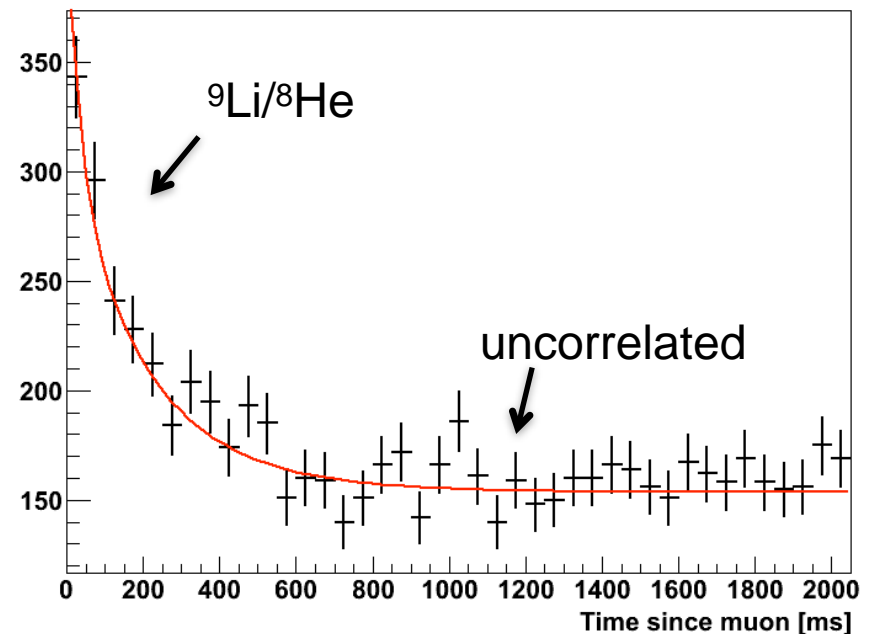
${}^9\text{Li}$ :  $\tau_{1/2} = 178$  ms,  $Q = 13.6$  MeV

${}^8\text{He}$ :  $\tau_{1/2} = 119$  ms,  $Q = 10.6$  MeV

- Generated by cosmic rays
- Long-lived
- Mimic antineutrino signal

This background is directly measured by fitting the distribution of IBD candidates vs. time since last muon.

${}^9\text{Li} / {}^8\text{He}$  Decay

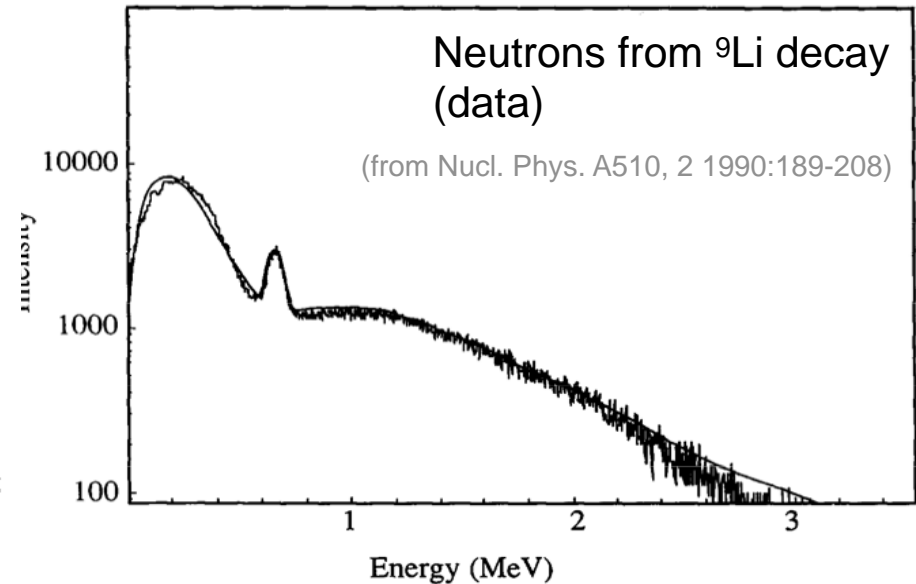
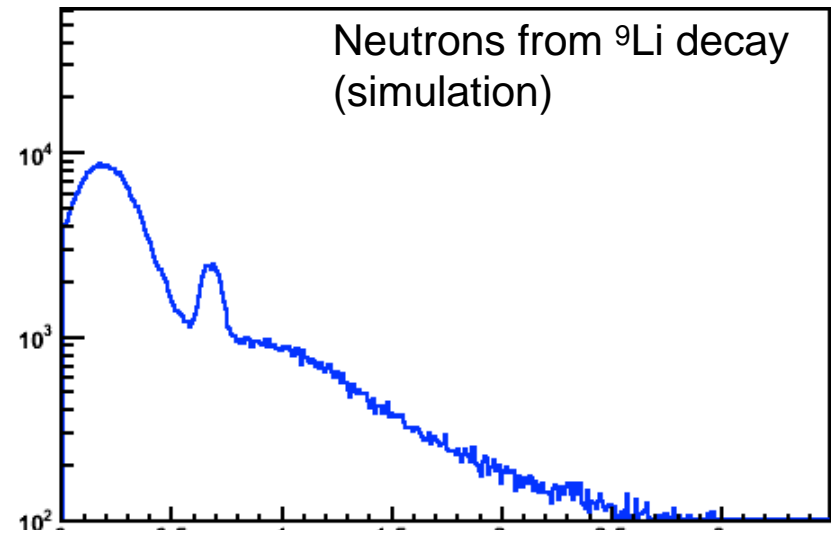
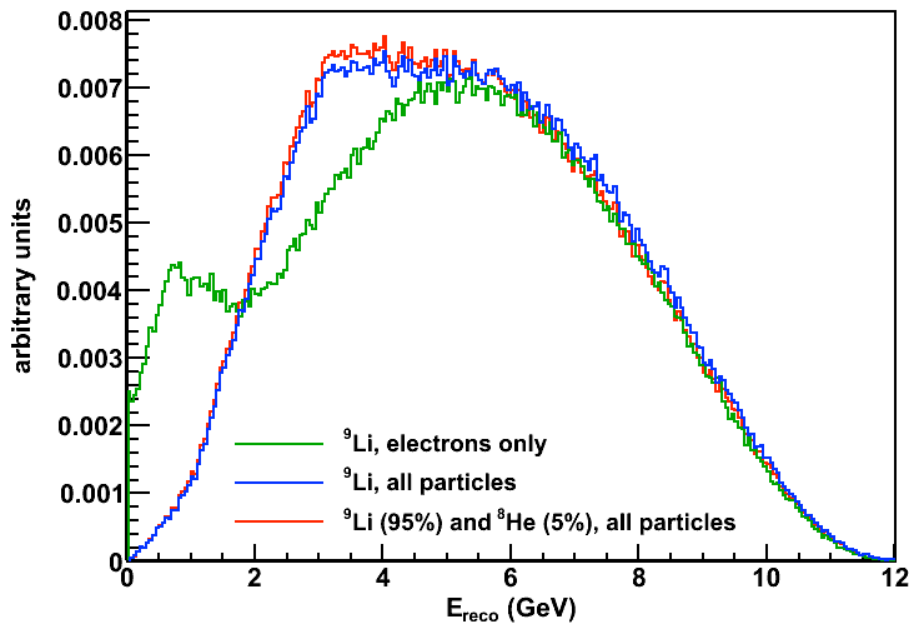


Analysis muon veto cuts control B/S to  $\sim 0.3 \pm 0.1\%$ .

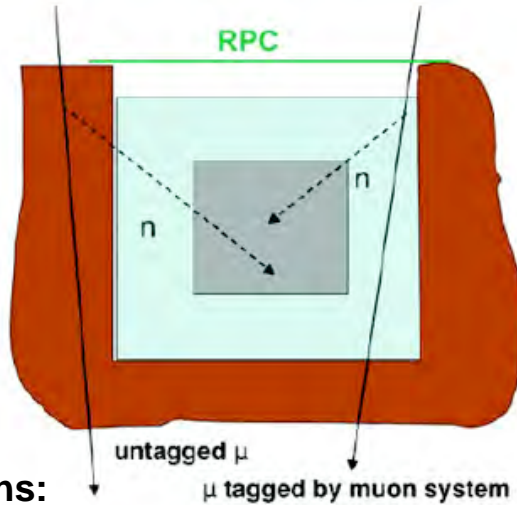
# Background: $\beta$ -n decay (Shape)

Shape for  ${}^9\text{Li}$  and  ${}^8\text{He}$  is predicted from a simulation benchmarked with external data and which accounts for all daughter particles.

Uncertainty in shape is conservatively accounted for by varying the  ${}^9\text{Li}/({}^9\text{Li}+{}^8\text{He})$  ratio, as well as the parameters of the detector response model.



# Background: Fast neutrons



## Fast Neutrons:

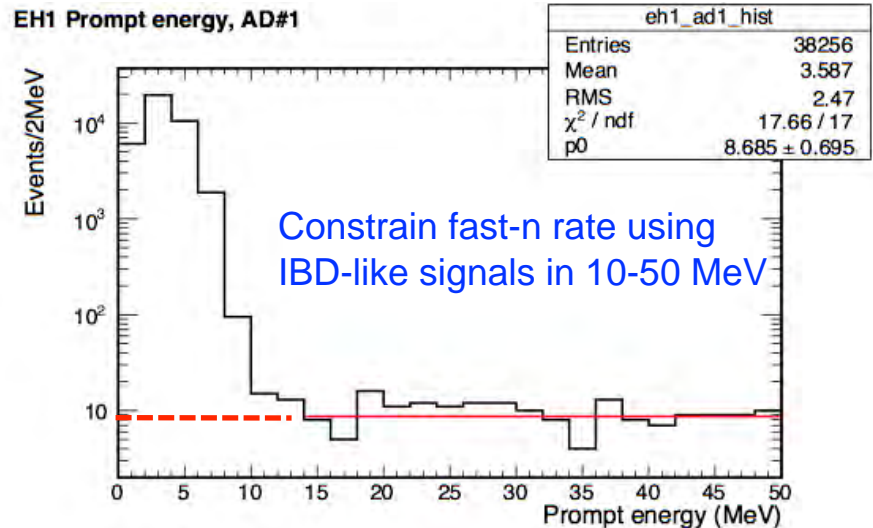
Energetic neutrons produced by cosmic rays (inside and outside of muon veto system)

## Mimics antineutrino (IBD) signal:

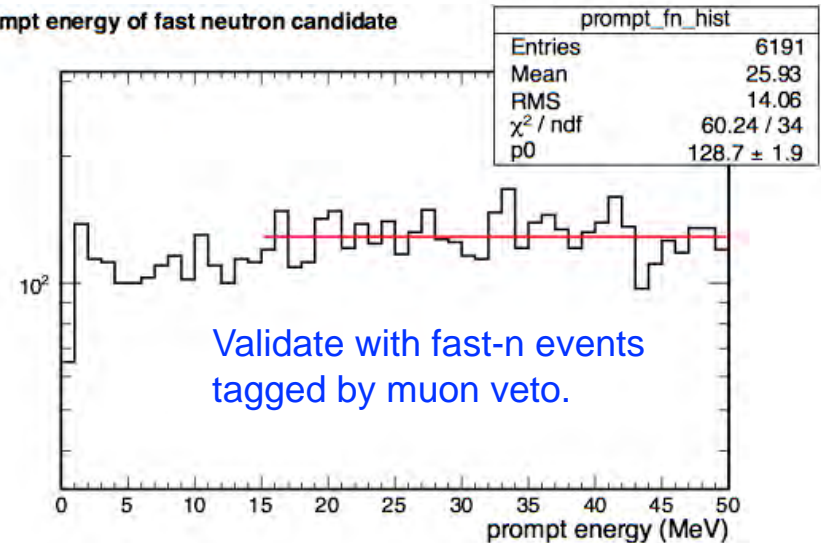
- Prompt: Neutron collides/stops in target
- Delayed: Neutron captures on Gd

Analysis muon veto cuts control B/S to 0.06% (0.1%) of far (near) signal.

EH1 Prompt energy, AD#1



prompt energy of fast neutron candidate



# Signal and Background Summary

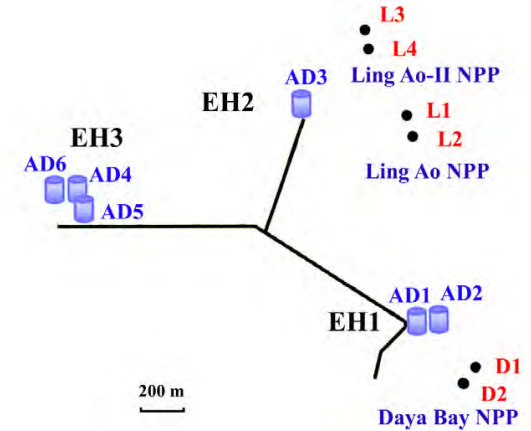
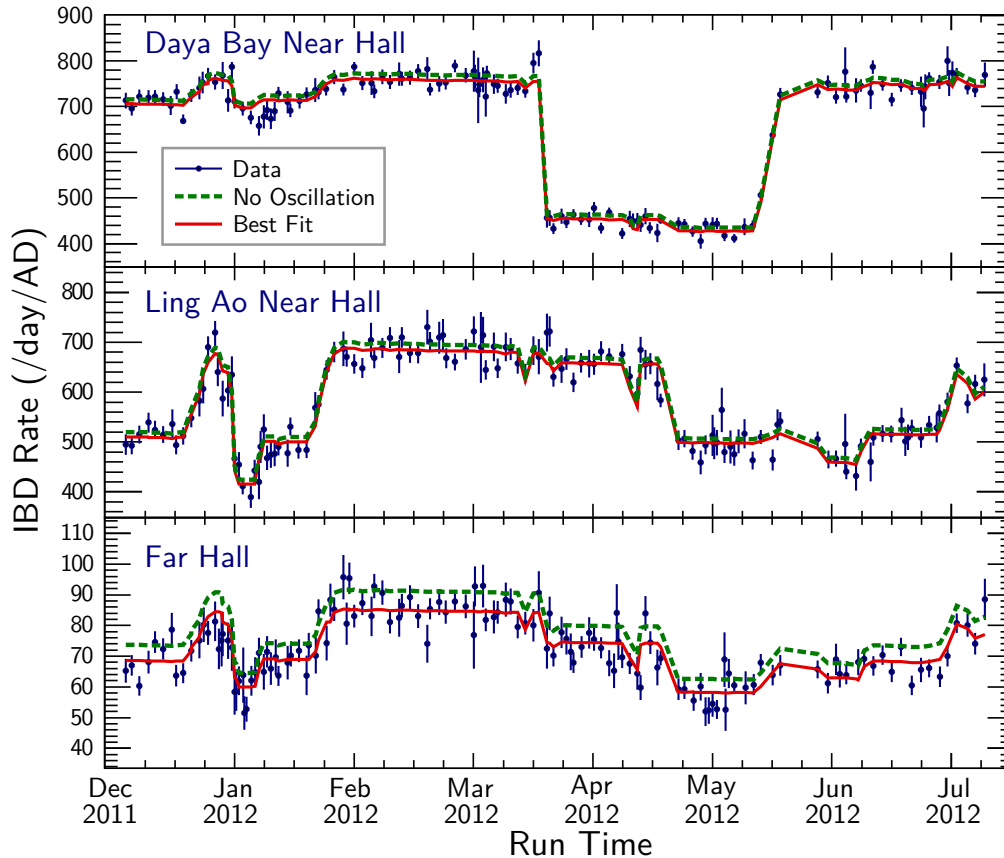
	Near Halls			Far Hall		
	AD 1	AD 2	AD 3	AD 4	AD 5	AD 6
IBD candidates	101290	102519	92912	13964	13894	13731
DAQ live time (days)	191.001		189.645	189.779		
Efficiency $\epsilon_\mu \cdot \epsilon_m$	0.7957	0.7927	0.8282	0.9577	0.9568	0.9566
Accidentals (per day)*	$9.54 \pm 0.03$	$9.36 \pm 0.03$	$7.44 \pm 0.02$	$2.96 \pm 0.01$	$2.92 \pm 0.01$	$2.87 \pm 0.01$
Fast-neutron (per day)*	$0.92 \pm 0.46$		$0.62 \pm 0.31$	$0.04 \pm 0.02$		
${}^9\text{Li}/{}^8\text{He}$ (per day)*	$2.40 \pm 0.86$		$1.2 \pm 0.63$	$0.22 \pm 0.06$		
Am-C corr. (per day)*	$0.26 \pm 0.12$					
${}^{13}\text{C}{}^{16}\text{O}$ backgr. (per day)*	$0.08 \pm 0.04$	$0.07 \pm 0.04$	$0.05 \pm 0.03$	$0.04 \pm 0.02$	$0.04 \pm 0.02$	$0.04 \pm 0.02$
IBD rate (per day)*	$653.30 \pm 2.31$	$664.15 \pm 2.33$	$581.97 \pm 2.07$	$73.31 \pm 0.66$	$73.03 \pm 0.66$	$72.20 \pm 0.66$

\*Background and IBD rates were corrected for the efficiency of the muon veto and multiplicity cuts  $\epsilon_\mu \cdot \epsilon_m$

Collected more than 300k antineutrino interactions

- Consistent rates for side-by-side detectors
- Uncertainties still dominated by statistics

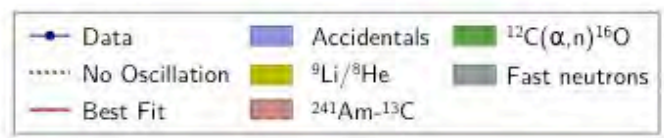
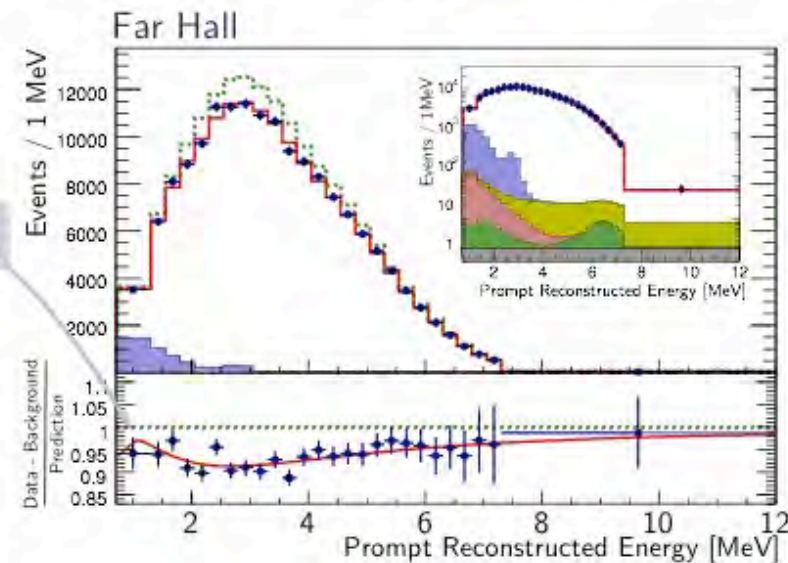
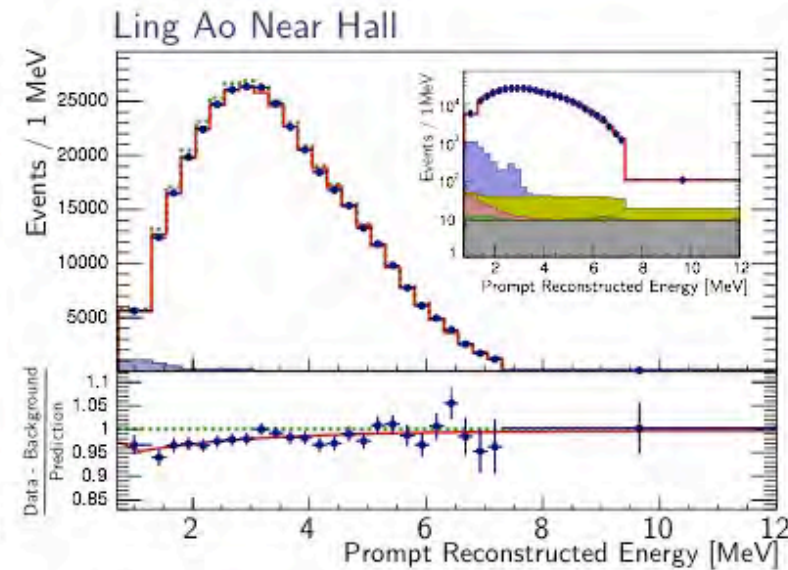
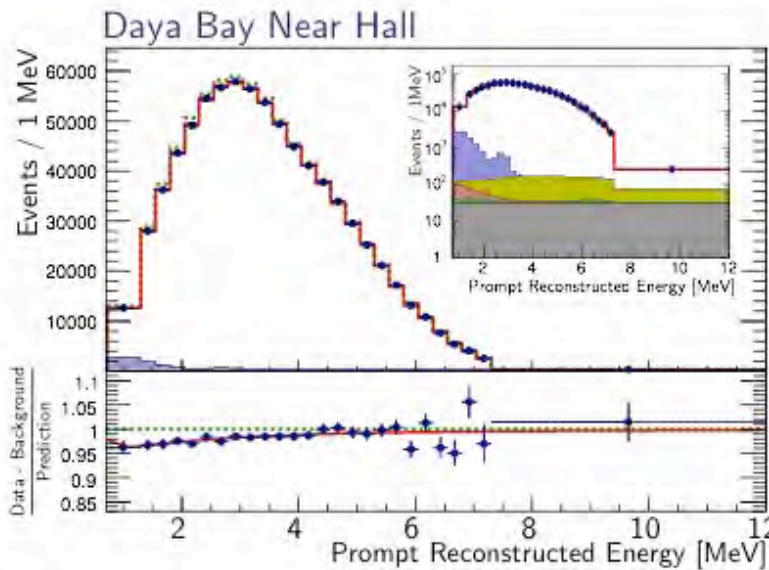
# Antineutrino Rate vs Time



Detected rate strongly correlated with reactor flux expectations

- Predicted rate assumes no oscillation
- Absolute normalization determined by fit to data
- Normalization within a few percent of expectations

# Prompt IBD Spectra



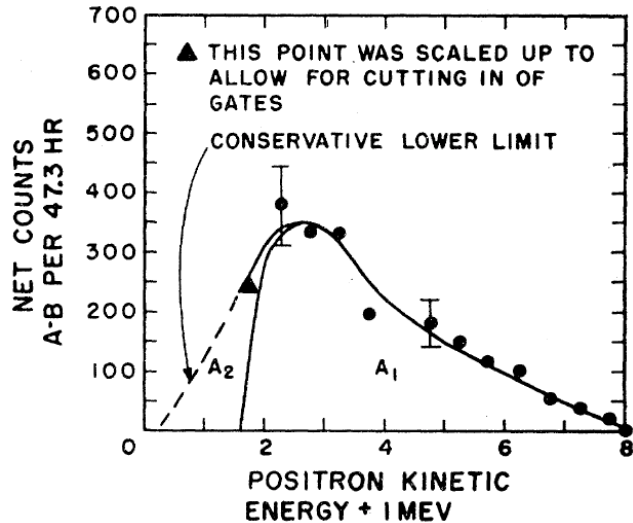
Spectral distortion  
consistent with oscillation

Shape distortion from energy losses in acrylic

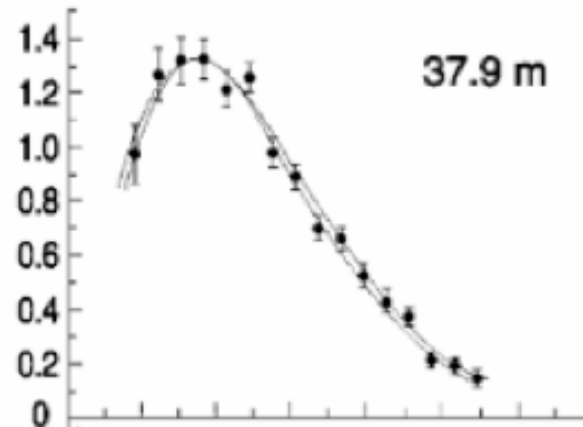
- Both background and predicted no oscillation spectrum determined by best fit
- Errors statistical only

# Towards a Precision Reactor Spectrum

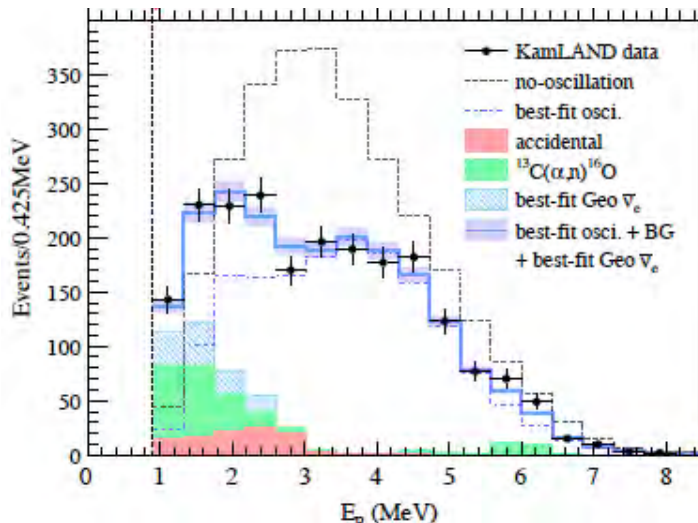
Reines 1959



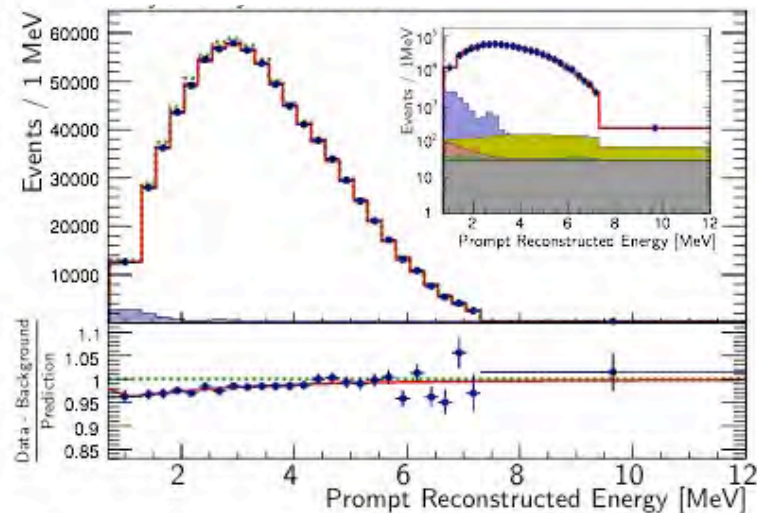
Goesgen 1986



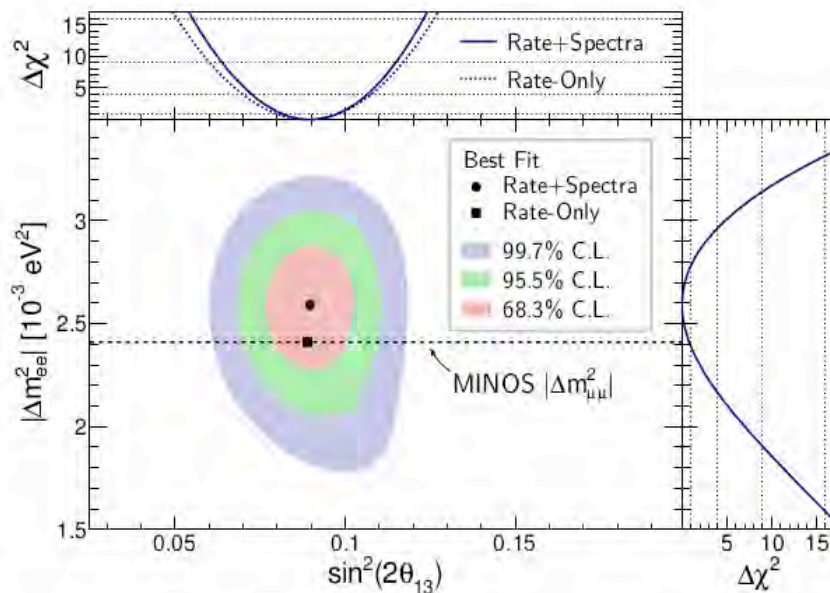
KamLAND 2010



Daya Bay (> 300,000 events)



# Rate+Spectra Oscillation Analysis



$$\sin^2 2\theta_{13} = 0.090^{+0.008}_{-0.009}$$

$$|\Delta m_{ee}^2| = 2.59^{+0.19}_{-0.20} \cdot 10^{-3} \text{eV}^2$$

$$\chi^2/N_{\text{DoF}} = 162.7/153$$

Strong confirmation of oscillation-interpretation of observed  $\bar{\nu}_e$  deficit

Normal MH  $\Delta m_{32}^2$   
[ $10^{-3} \text{eV}^2$ ]

Inverted MH  $\Delta m_{32}^2$   
[ $10^{-3} \text{eV}^2$ ]

From Daya Bay  $\Delta m_{ee}^2$

$2.54^{+0.19}_{-0.20}$

$-2.64^{+0.19}_{-0.20}$

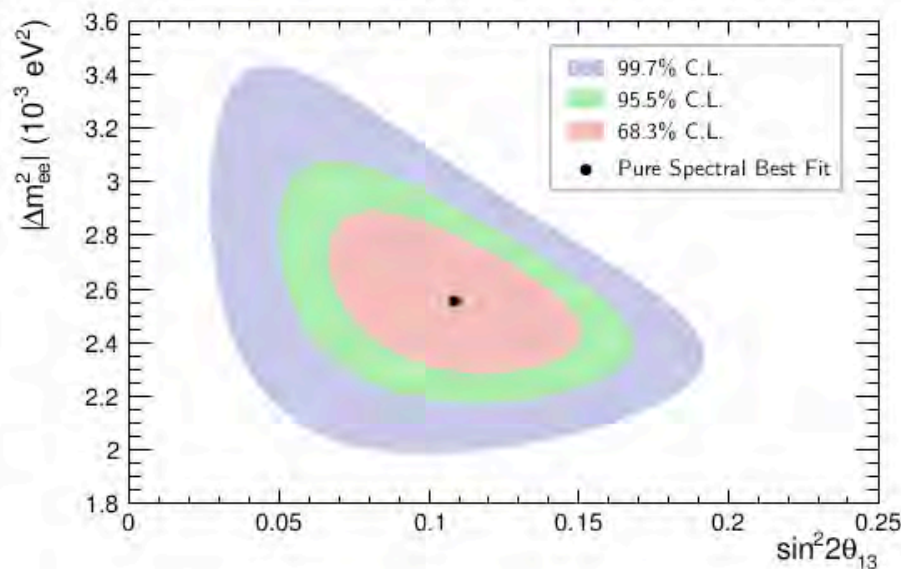
From MINOS  $\Delta m_{\mu\mu}^2$

$2.37^{+0.09}_{-0.09}$

$-2.41^{+0.11}_{-0.09}$

A. Radovic,  
DPF2013





$$\sin^2 2\theta_{13} = 0.108 \pm 0.028$$

$$|\Delta m_{ee}^2| = 2.55_{-0.18}^{+0.21} \cdot 10^{-3} \text{ eV}^2$$

$$\chi^2/N_{\text{DoF}} = 161.2/148$$

$\theta_{13} = 0$  can be excluded at  $> 3\sigma$  from spectral information alone

■ For each AD, total event prediction fixed to observed data:

1  $\theta_{13}$  free-floating:  $\chi^2/N_{\text{DoF}} = 161.2/148$

2  $\theta_{13} = 0$ :  $\chi^2/N_{\text{DoF}} = 178.5/146$

$\Rightarrow \Delta\chi^2/N_{\text{DoF}} = 17.3/2$ , corresponding to  $p = 1.75 \cdot 10^{-4}$


# A Comment on $\Delta m^2$

Short-baseline reactor experiments insensitive to neutrino mass hierarchy.

Cannot discriminate two frequencies contributing to oscillation:  $\Delta m_{31}^2$ ,  $\Delta m_{32}^2$

One effective oscillation frequency is measured:

$$P_{\bar{\nu}_e \rightarrow \bar{\nu}_e} = 1 - \sin^2 2\theta_{13} \sin^2 \left( \Delta m_{ee}^2 \frac{L}{4E} \right) - \sin^2 2\theta_{12} \cos^4 2\theta_{13} \sin^2 \left( \Delta m_{21}^2 \frac{L}{4E} \right)$$


$$\sin^2 \left( \Delta m_{ee}^2 \frac{L}{4E} \right) \equiv \cos^2 \theta_{12} \sin^2 \left( \Delta m_{31}^2 \frac{L}{4E} \right) + \sin^2 \theta_{12} \sin^2 \left( \Delta m_{32}^2 \frac{L}{4E} \right)$$

Result can be easily related to actual mass splitting, based on true hierarchy:

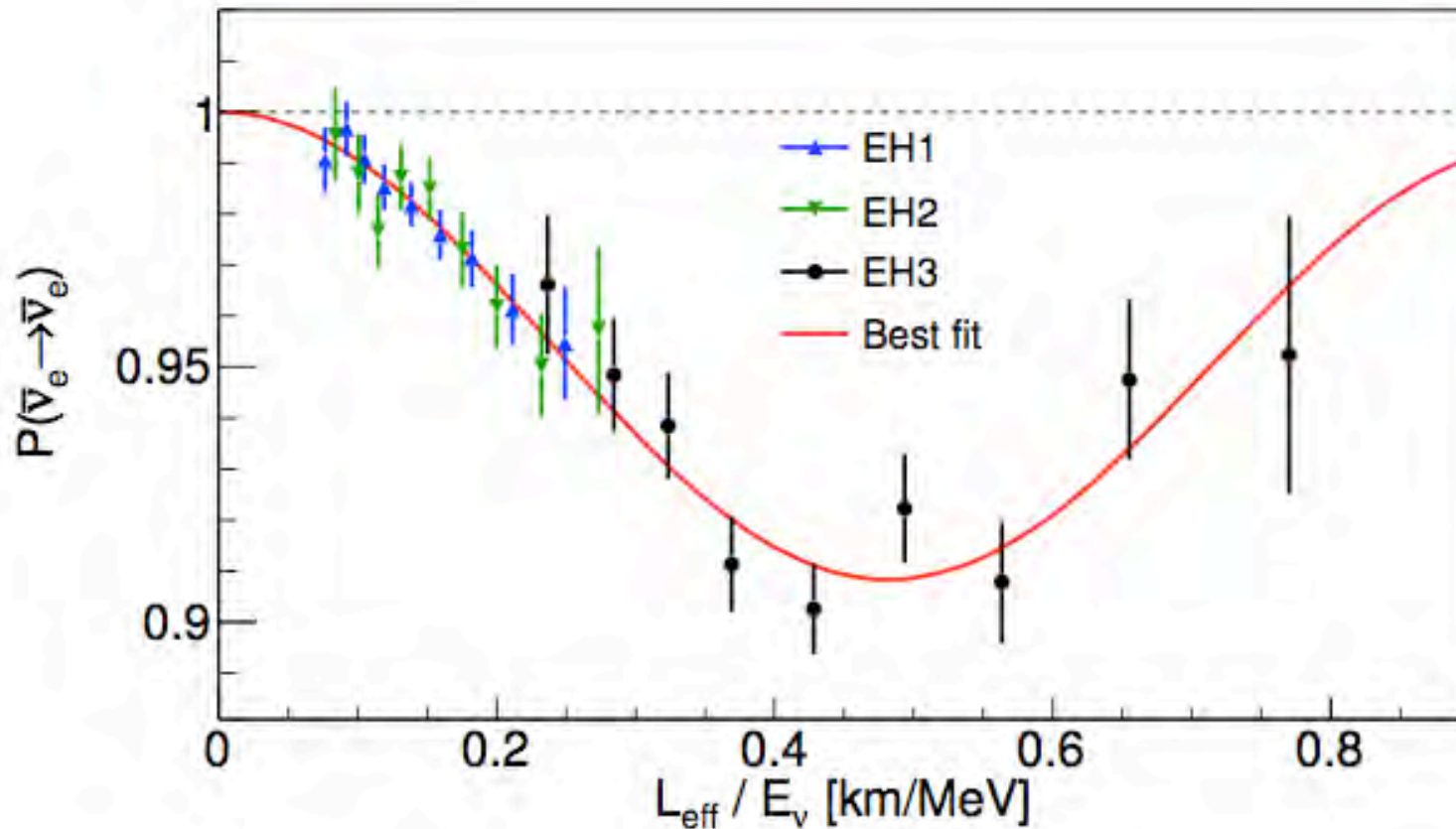
$$|\Delta m_{ee}^2| \simeq |\Delta m_{32}^2| \pm 5.21 \times 10^{-5} \text{eV}^2$$

+: Normal Hierarchy  
-: Inverted Hierarchy

Hierarchy discrimination requires  $\sim 2\%$  precision on both  $\Delta m_{ee}^2$  and  $\Delta m_{\mu\mu}^2$

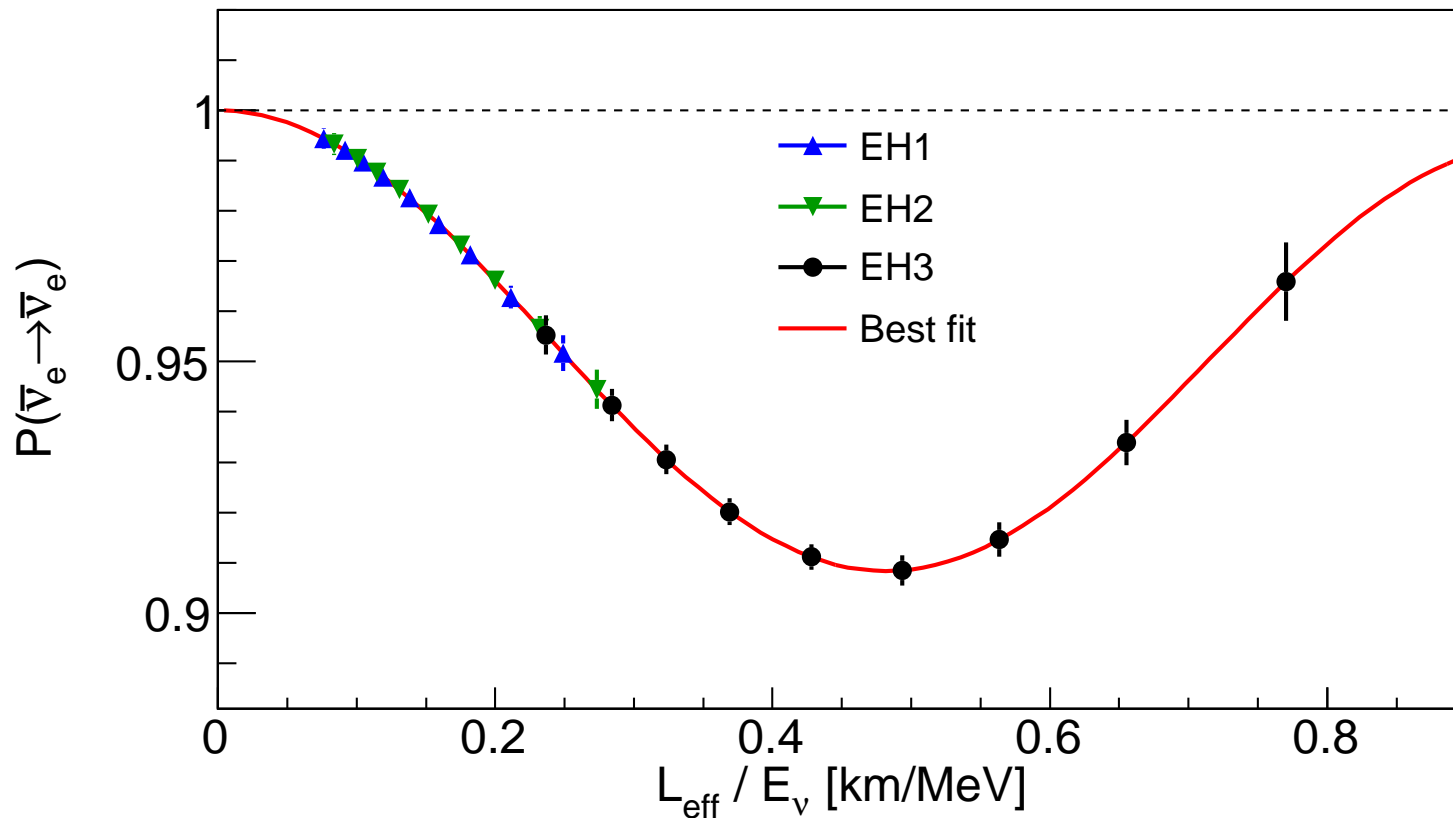
# L/E Oscillation

## Energy and Baseline Dependence of Oscillation Effect



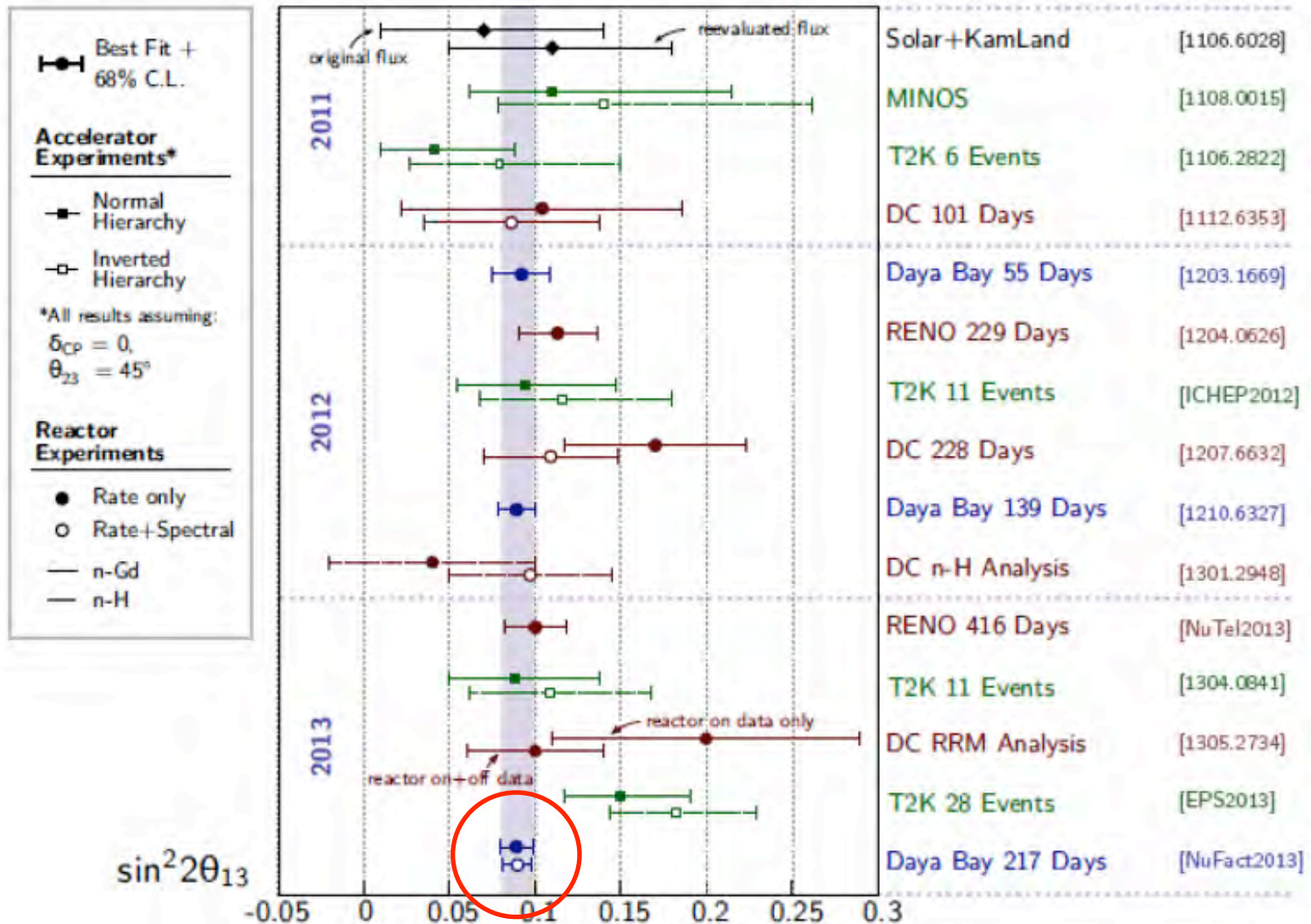
now

## Energy and Baseline Dependence of Oscillation Effect



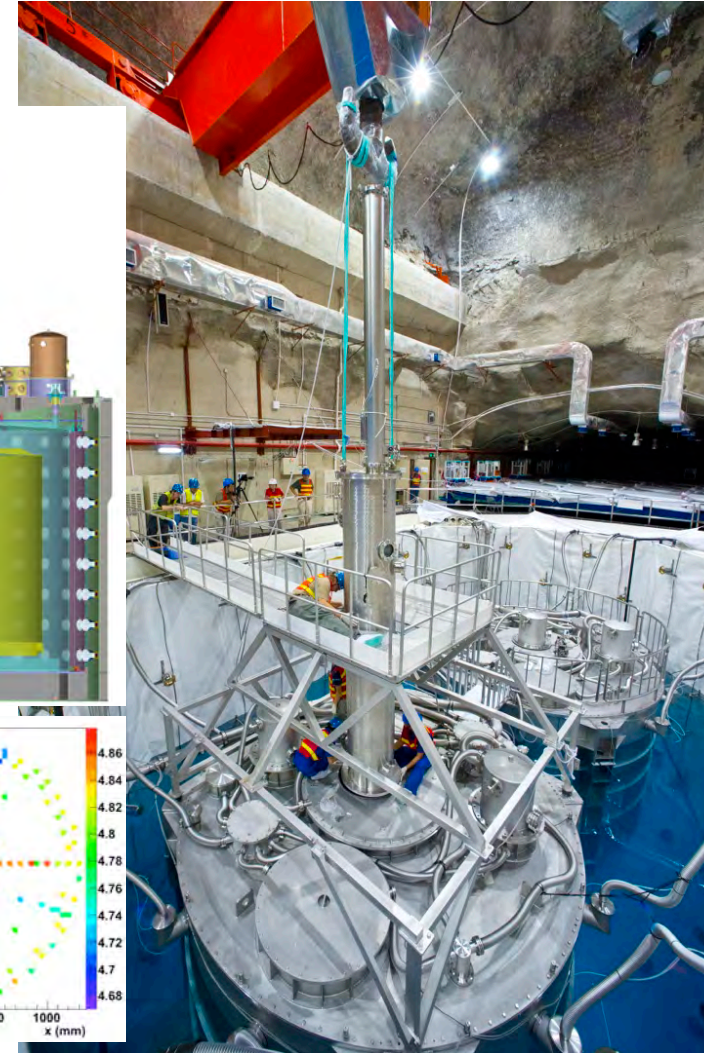
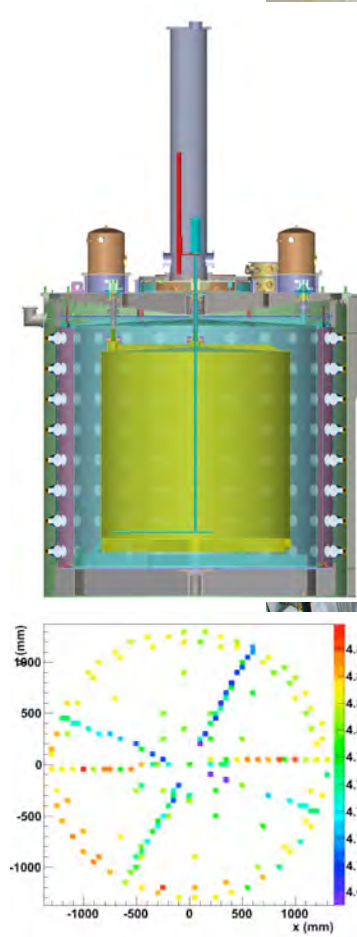
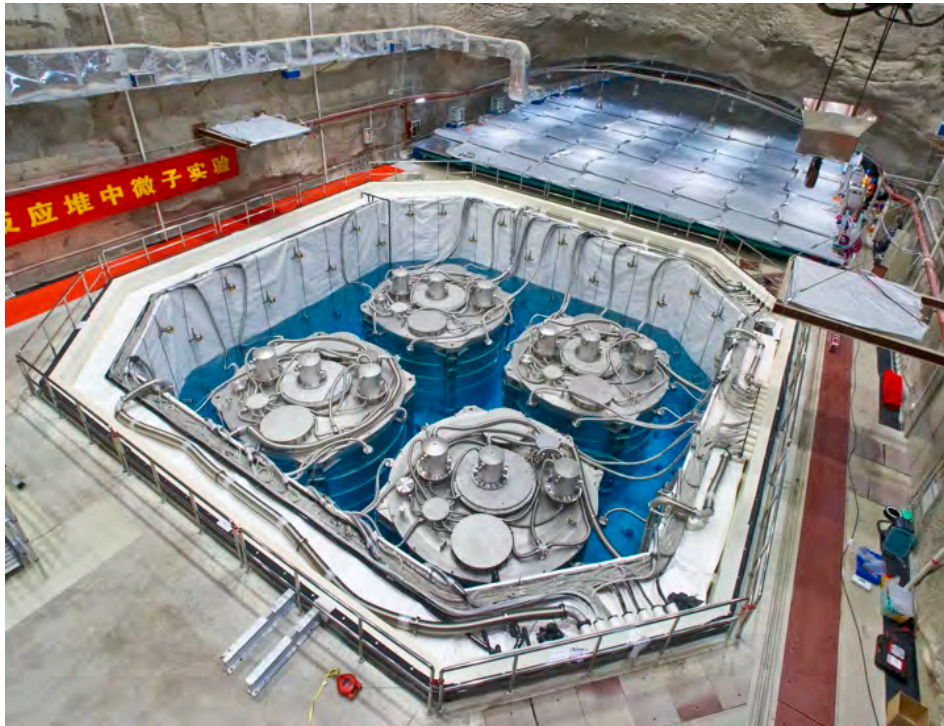
in FY17

# Global Comparison of $\theta_{13}$ Measurements

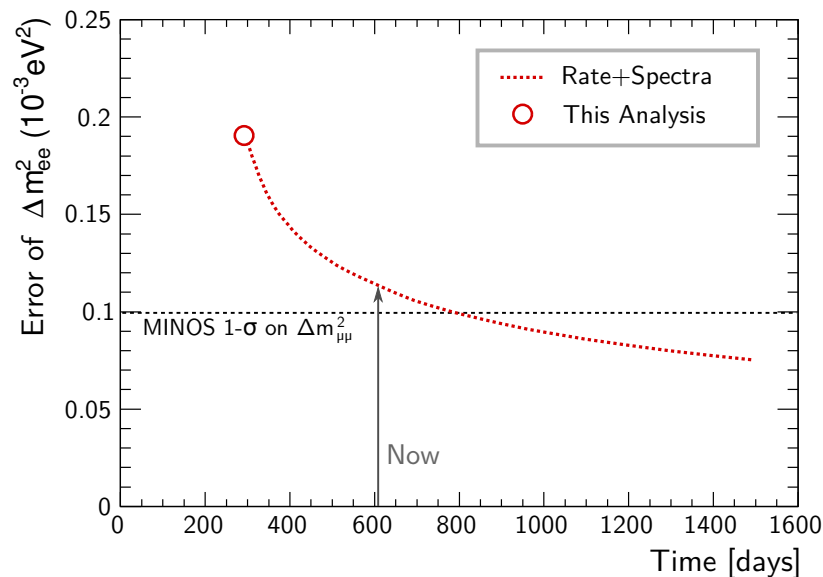
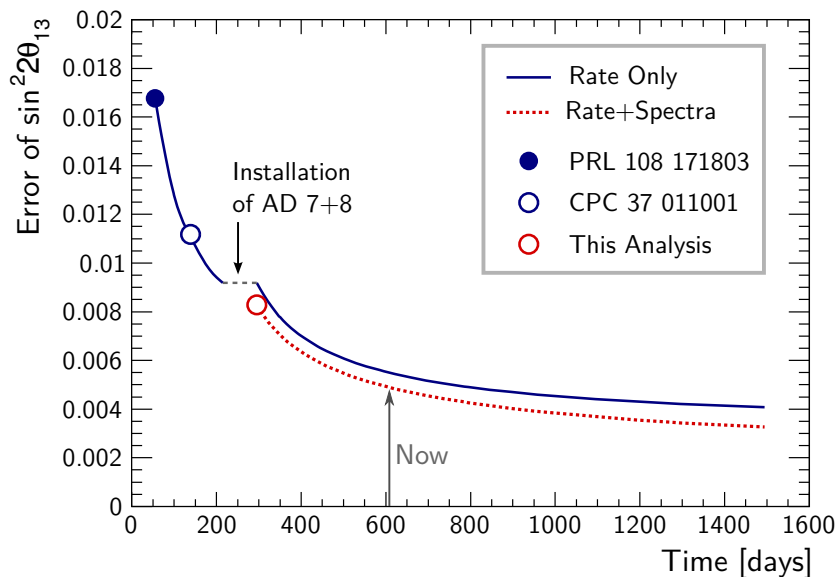


## Installation of Final Antineutrino Detectors

## Full Volume Calibration



## Improved precision on oscillation parameters



- Statistics contribute 73% (65%) to total uncertainty in  $\sin^2 2\theta_{13}$  ( $|\Delta m^2_{ee}|$ )
- Major systematics:
  - $\theta_{13}$ : Relative + absolute energy, and relative efficiencies
  - $|\Delta m^2_{ee}|$ : Relative energy model, relative efficiencies, and backgrounds
- Precision of mass splitting measurement closing in on results from  $\mu$  flavor sector

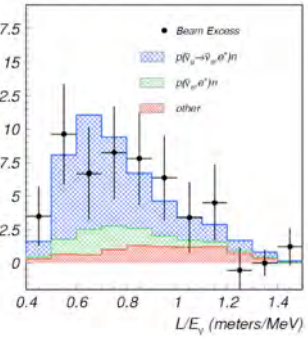
Measure absolute reactor neutrino flux and spectrum

Cosmogenic Backgrounds

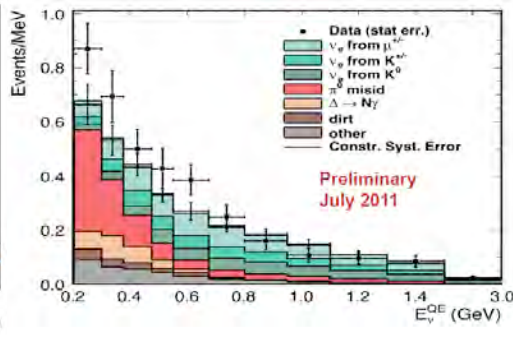
Supernova Neutrinos

# Neutrino Anomalies

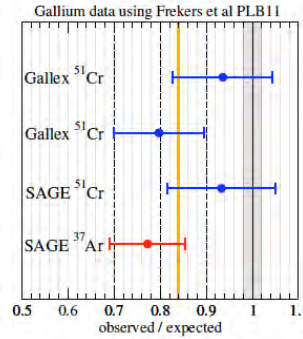
LSND



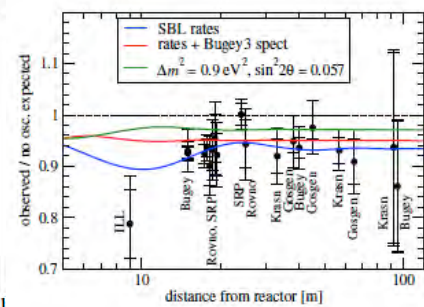
MiniBoone



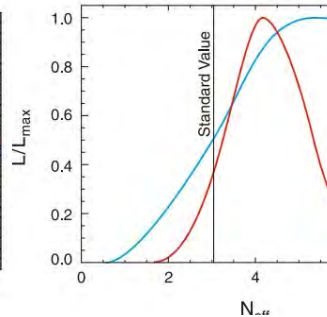
Ga Source



Reactor



Cosmology (WMAP)



## Anomalies in 3-ν interpretation of global oscillation data

LSND ( $\bar{\nu}_e$  appearance)

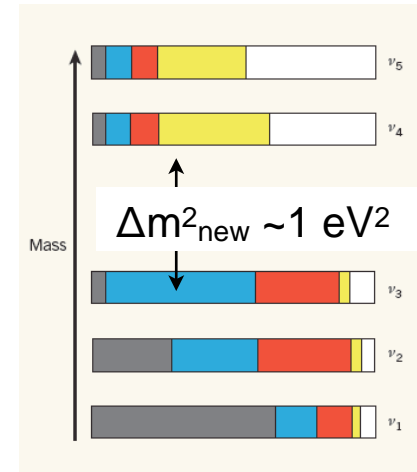
MiniBoone ( $\nu_e$  appearance)

Ga anomaly

Reactor anomaly ( $\bar{\nu}_e$  disappearance)

## Cosmology suggests higher radiation density

$$N_{\text{eff}} > 3$$

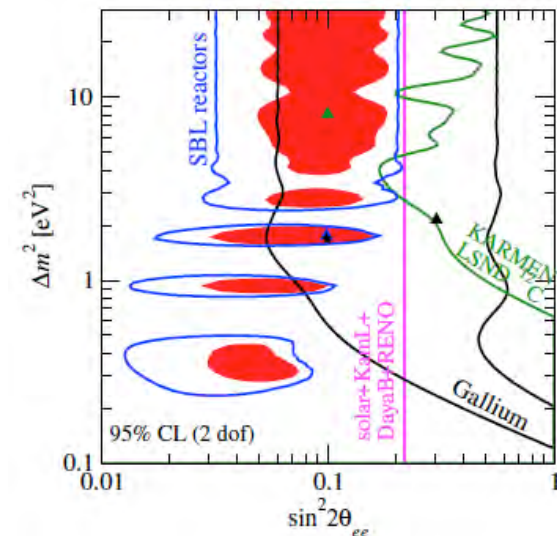
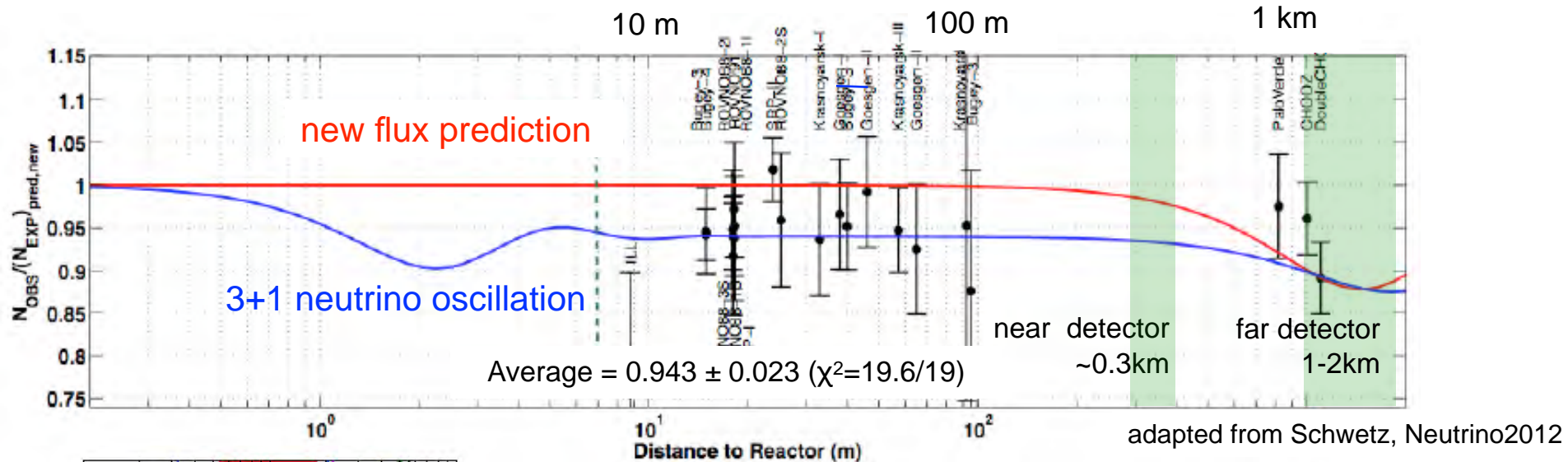


new oscillation signal requires  $\Delta m^2 \sim O(1\text{eV}^2)$  and  $\sin^2 2\theta > 10^{-3}$   
 systematics or experimental effect?  $\rightarrow$  need to test effects



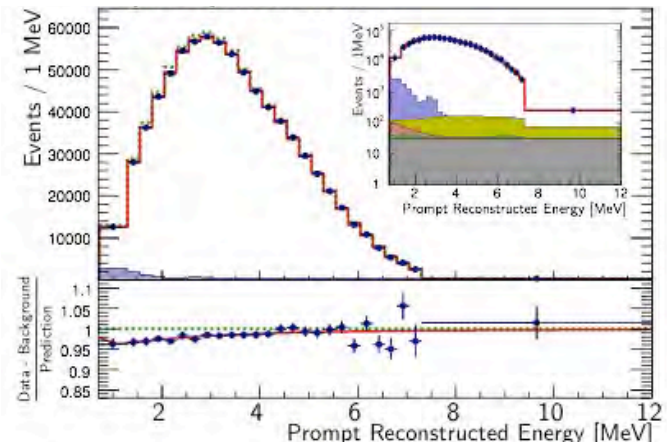
# Reactor Fluxes and “Anomaly”

Reactor  $\theta_{13}$  experiments cannot directly search for short-baseline oscillations



at  $\sim 1\text{km}$  reactor  $\theta_{13}$  experiments probe overall suppression

Precision measurement of spectral shape can reveal new physics independent of normalization



# Summary



For > 60 years reactor experiments have played an important role in neutrino physics, in both discoveries and precision measurements.

Reactors are flavor pure sources of  $\bar{\nu}_e$ .

Current reactor experiments (**L~1-2km**) provide precision data on  $\theta_{13}$ , and **reactor antineutrino spectra**.

The Daya Bay Experiment has reported the first direct measurement of the short-distance electron antineutrino oscillation frequency:

$$|\Delta m_{ee}^2| = 2.59_{-0.20}^{+0.19} \times 10^{-3} \text{eV}^2$$

The measurement has also produced the most precise estimate of the mixing angle:

$$\sin^2(2\theta_{13}) = 0.090_{-0.009}^{+0.008}$$

There is more to come... stay tuned!

End